

On the Energy-Efficient Deployment for Ultra-Dense Heterogeneous Networks with NLoS and LoS Transmissions

Bin Yang, *Student Member, IEEE*, Guoqiang Mao, *Fellow, IEEE*, Xiaohu Ge, *Senior Member, IEEE*, Ming Ding, *Senior Member, IEEE*, Xuan Yang

Abstract—We investigate network performance of ultra-dense heterogeneous networks (HetNets) and study the maximum energy-efficient base station (BS) deployment incorporating probabilistic non-line-of-sight (NLoS) and line-of-sight (LoS) transmissions. First, we develop an analytical framework with the maximum instantaneous received power (MIRP) and the maximum average received power (MARP) association schemes to model the coverage probability and related performance metrics, *e.g.*, the potential throughput (PT) and the energy efficiency (EE). Second, we formulate two optimization problems to achieve the maximum energy-efficient deployment solution with specific service criteria. Simulation results show that there are tradeoffs among the coverage probability, the total power consumption, and the EE. To be specific, the maximum coverage probability with ideal power consumption is superior to that with practical power consumption when the total power constraint is small and inferior to that with practical power consumption when the total power constraint becomes large. Moreover, the maximum EE is a decreasing function with respect to the coverage probability constraint.

Index Terms—Ultra-Dense HetNets, non-line-of-sight (NLoS), line-of-sight (LoS), Poisson point process (PPP), energy efficiency (EE), optimization, cell association scheme.

I. INTRODUCTION

Ultra-dense deployment of small cell base stations (BSs), relay nodes, and distributed antennas is considered as a de facto solution for realizing the significant performance improvements needed to accommodate the overwhelming future

Manuscript received September 7, 2017; revised December 8, 2017 ; accepted January 21, 2018. Date of publication xx xx, xx; date of current version xx xx, xx. The authors would like to acknowledge the support from the NFSC Major International Joint Research Project under Grant 61210002, the China International Joint Research Center of Green Communications and Networking under Grant 2015B01008, and the Hubei Provincial Science and Technology Department under Grant 2016AHB006. This research is partially supported by the EU FP7-PEOPLE-IRSES, the project acronym CROWN under Grant 610524, the EU H2020-ICT-2016-INT, the project acronym EXCITING under Grant 723227, and the China Scholarship Council (CSC no. 201506160107).

Copyright (c) 2015 IEEE. Personal use of this material is permitted. However, permission to use this material for any other purposes must be obtained from the IEEE by sending a request to pubs-permissions@ieee.org.

Correspondence author: Prof. Xiaohu Ge (Email: xhge@mail.hust.edu.cn, Tel: +86-27-87557941 ext 822).

Bin Yang, Xiaohu Ge and Xuan Yang are with the School of Electronic Information and Communications, Huazhong University of Science and Technology, China (Email: yangbin@hust.edu.cn, xhge@mail.hust.edu.cn, xuan_yan9@163.com).

Guoqiang Mao is with the School of Computing and Communication, The University of Technology Sydney, Australia (e-mail: g.mao@ieee.org).

Ming Ding is with Data61, CSIRO, Australia (Email: ming.ding@data61.csiro.au).

mobile traffic demand [1]. Traditional network expansion techniques like cell splitting are often utilized by telecom operators to achieve the expected throughput, which is less efficient and proven not to keep up with the pace of traffic proliferation in the near future. Heterogeneous networks (HetNets) then become a promising and attractive network architecture to alleviate the problem. “HetNets” is a broad term that refers to the coexistence of different networks (*e.g.*, traditional macrocells and small cell networks like femtocells and picocells), each of them constituting a network tier. Due to differences in deployment, BSs in different tiers may have different transmit powers, radio access technologies, fading environments and spatial densities. HetNets are envisioned to change the existing network architectures and have been introduced in the LTE-Advanced standardization [2, 3].

Massive work has been done in HetNets scenario mainly related to cell association scheme [4–6], cache-enabled networks [7], physical layer security [8], *etc.* In [4], the pertinent user association algorithms designed for HetNets, massive MIMO networks, mmWave scenarios and energy harvesting networks have been surveyed for the future fifth generation (5G) networks. Bethanabhotla *et al.* [5] investigated the optimal user-cell association problem for massive MIMO HetNets and illustrated how massive MIMO could also provide non-trivial advantages at the system level. The joint downlink cell association and wireless backhaul bandwidth allocation in a two-tier HetNet is studied in [6]. In [7], Yang *et al.* aimed to model and evaluate the performance of the wireless HetNet where the radio access network (RAN) caching and device-to-device (D2D) caching coexist. The physical layer security of HetNets where the locations of all BSs, mobile users (MUs) and eavesdroppers are modeled as independent homogeneous PPPs in [8].

From the mobile operators point of view, the commercial viability of network densification depends on the underlying capital and operational expenditure [9]. While the former cost may be covered by taking up a high volume of customers, with the rapid rise in the price of energy, and given that BSs are particularly power-hungry, energy efficiency (EE) has become an increasingly crucial factor for the success of dense HetNets [10]. Recently, loads of work [11–15] has investigated the EE in the 5G network scenarios. In [11], Niu *et al.* investigated the problem of minimizing the energy consumption via optimizing concurrent transmission scheduling and power control for the mmWave backhauling of small cells densely deployed

in HetNets. A self-organized cross-layer optimization for enhancing the EE of the D2D communications without creating harmful impact on other tiers by employing a non-cooperative game in a three-tier HetNet is proposed in [12]. To jointly optimize the EE and video quality, Wu *et al.* [13] presented an energy-quality aware bandwidth aggregation scheme. In [14], Yang *et al.* investigated the energy-efficient resource allocation problem for downlink heterogeneous OFDMA networks. The mobile edge computing offloading mechanisms are studied in 5G HetNets [15].

Different from most prior work analyzing network performance where the propagation path loss between the BSs and the MUs follows the same power-law model, in this paper we consider the co-existence of both non-line-of-sight (NLoS) and line-of-sight (LoS) transmissions, which frequently occur in *urban areas*. More specifically, for a randomly selected MU, BSs deployed according to a homogeneous Poisson point process (PPP) are divided into two categories, *i.e.*, NLoS BSs and LoS BSs, depending on the distance between BSs and MUs. It is well known that LoS transmission may occur when the distance between a transmitter and a receiver is small, and NLoS transmission is common in office environments and central business districts. Moreover, as the trend of ultra-dense network deployment, the distance between a transmitter and a receiver decreases, the probability that a LoS path exists between them increases, thereby causing a transition from NLoS transmission to LoS transmission with a higher probability [16]. In this context, Ding *et al.* [16] studied the coverage and capacity performance by using a multi-slope path loss model incorporating probabilistic NLoS and LoS transmissions. The coverage and capacity performance in millimeter wave cellular networks are studied in [17–19]. In [17], a three-state statistical model for each link was assumed, in which a link can either be in an NLoS, LoS or an outage state. In [18], self-backhauled millimeter wave cellular networks are characterized assuming a cell association scheme based on the smallest path loss. However, both [17] and [18] assume a noise-limited network, ignoring inter-cell interference, which may not be very practical since modern wireless networks work in the interference-limited region. In [19], the coverage probability and capacity were calculated in a millimeter wave cellular network based on the smallest path loss cell association model assuming multi-path fading modeled as Nakagami- m fading, respectively. However, shadowing was ignored in their models, which may not be very practical for an ultra-dense heterogeneous network.

In contrast to prior work, we investigate the HetNets in a more realistic scenario, *i.e.*, NLoS and LoS transmissions in desired signal and interference signal are both considered. Besides, we also explore the optimal BS deployment under the quality of service (QoS) constraint. The main contributions of this paper are summarized as follows:

- 1) **A unified framework:** We propose a unified framework, in which the user association strategies based on the maximum instantaneous received power (MIRP) and the maximum average received power (MARP) can be studied, assuming log-normal shadowing, Rayleigh fading and incorporating probabilistic NLoS and LoS

transmissions.

- 2) **Performance optimization:** We formulate two optimization problems under different QoS constraints, *i.e.*, the maximal total power consumption and the minimal coverage probability. Utilizing solutions of the above optimization problems, the maximum energy-efficient BS deployment is obtained.
- 3) **Network design insights:** We compare the optimal BS deployment strategies in different network scenarios, *i.e.*, assuming the fixed transmit power, the density-dependent transmit power, with and without considering the static power consumption in BSs. Through our results, the maximum coverage probability with ideal power consumption is superior to that with practical power consumption when the total power constraint is small and inferior to that with practical power consumption when the total power constraint becomes large. Moreover, the maximum EE is a decreasing function with respect to the coverage probability constraint.

The remainder of this paper is organized as follows. Section II introduces the system model, network assumptions, and performance metrics. In section III, the coverage probability, the potential throughput (PT) and the EE of the HetNets are derived with the MIRP and the MARP association schemes, respectively. In Section IV, two optimization problems for energy-efficient BS deployment are formulated. In Section V, the analytical results are validated via Monte Carlo simulations. Besides, the insights of BS deployment are studied. Finally, Section VI concludes this paper and discusses possible future work.

II. SYSTEM MODEL

In this paper, a K -tier HetNet is considered, which consists of macrocells, picocells, femtocells, *etc.* BSs of each tier are assumed to be spatially distributed on the infinite plane and locations of BSs follow independent homogeneous Poisson point processes (HPPPs) denoted by $\Phi_k = \{\mathbf{X}_{k,i}\}$ with a density (*aka* intensity) λ_k , $k \in \{1, 2, \dots, K\} \stackrel{\text{def}}{=} \mathcal{K}^1$, where $\mathbf{X}_{k,i}$ denotes the location of BS in the k -th tier. MUs are deployed according to another independent HPPP denoted by Φ_u with a density λ_u ($\lambda_u \gg \lambda_k$). BSs belonging to the same tier transmit using the same constant power P_k and sharing the same bandwidth. Besides, within a cell assume that each MU uses orthogonal multiple access method to connect to a serving BS for downlink and uplink transmissions and therefore there is no intra-cell interference in the analysis of our paper. However, adjacent BSs which are not serving the connected MU may cause inter-cell interference which is the main focus of this paper. It is further assumed that each MU can possibly associate with a BS belonging to any tier, *i.e.*, *open access* policy is employed.

Without loss of generality and from the Slivnyak's Theorem [20], we consider the *typical MU* which is usually assumed to be located at the origin, as the focus of our performance analysis.

¹ $x \stackrel{\text{def}}{=} y$ means x is defined to be another name for y .

A. Signal Propagation Model

The long-distance signal attenuation in tier k is modeled by a monotone, non-increasing and continuous path loss function $l_k : [0, \infty) \mapsto [0, \infty)$ and l_k decays to zero asymptotically. The fast fading coefficient for the wireless link between a BS $\mathbf{X}_{k,i} \in \Phi_k$ and the typical MU is denoted as $h_{\mathbf{X}_{k,i}}$. $\{h_{\mathbf{X}_{k,i}}\}$ are assumed to be random variables which are mutually independent and identically distributed (i.i.d.) and also independent of BS locations $\{\mathbf{X}_{k,i}\}$, thus $h_{\mathbf{X}_{k,i}}$ can be denoted as h_k for the sake of simplicity. Similarly, the shadowing is denoted by g_k and particularly assume that it follows a log-normal distribution with zero mean and standard deviation σ . Note that the proposed model is general enough to account for various propagation scenarios with fast fading, shadowing, and different path loss models.

To characterize shadowing effect in urban areas which is a unique scenario in our analysis, both NLoS and LoS transmissions are incorporated. That is, if the visual path between a BS $\mathbf{X}_{k,i} \in \Phi_k$ and the typical MU is blocked by obstacles like buildings, trees, and even MUs, it is an NLoS transmission. Otherwise it is a LoS transmission. The occurrence of NLoS and LoS transmissions depend on various environmental factors, including geographical structure, distance, and cluster. In this work, a one-parameter distance-based NLoS/LoS transmission probability model is applied. That is,

$$p_k^{\text{NL}}(\|\mathbf{X}_{k,i}\|) + p_k^{\text{L}}(\|\mathbf{X}_{k,i}\|) = 1, \quad (1)$$

where $p_k^{\text{NL}}(\|\mathbf{X}_{k,i}\|)$ and $p_k^{\text{L}}(\|\mathbf{X}_{k,i}\|)$ denote the probability of the occurrence of NLoS and LoS transmissions, respectively, $\|\mathbf{X}_{k,i}\|$ is the distance between the BS $\mathbf{X}_{k,i}$ and the typical MU.

Regarding the mathematical form of $p_k^{\text{L}}(\|\mathbf{X}_{k,i}\|)$ (or $p_k^{\text{NL}}(\|\mathbf{X}_{k,i}\|)$), Blaunstein *et al.* [21] formulated $p_k^{\text{L}}(\|\mathbf{X}_{k,i}\|)$ as a negative exponential function, *i.e.*, $p_k^{\text{L}}(\|\mathbf{X}_{k,i}\|) = e^{-\kappa\|\mathbf{X}_{k,i}\|}$, where κ is a parameter determined by the density and the mean length of the blockages lying in the visual path between BSs and the typical MU. Bai *et al.* [22] extended Blaunstein's work by using random shape theory which shows that κ is not only determined by the mean length but also the mean width of the blockages. [17] and [19] approximated $p_k^{\text{L}}(\|\mathbf{X}_{k,i}\|)$ by using piece-wise functions and step functions, respectively. Ding *et al.* [16] considered $p_k^{\text{L}}(\|\mathbf{X}_{k,i}\|)$ to be a linear function and a two-piece exponential function, respectively; both are recommended by the 3GPP. It is important to note that the introduction of NLoS and LoS transmissions is essential to model practical networks, where a MU does not necessarily have to connect to the nearest BS. Instead, for many cases, MUs are associated with farther BSs with stronger signal strength.

It should be noted that the occurrence of NLoS and LoS transmissions is assumed to be independent for different BS-MU pairs. Though such assumption might not be entirely realistic (*e.g.*, NLoS transmission caused by a large obstacle may be spatially correlated), Bai *et al.* [19, 22] showed that the impact of the independence assumption on the SINR analysis is negligible.

For a specific tier k , note that from the viewpoint of the typical MU, each BS in the infinite plane \mathbb{R}^2 is either an NLoS BS or a LoS BS to the typical MU. Accordingly, a thinning procedure on points in the PPP Φ_k is performed to model the distributions of NLoS BSs and LoS BSs, respectively. That is, each BS in Φ_k will be kept if a BS has an NLoS transmission with the typical MU, thus forming a new point process denoted by Φ_k^{NL} . While BSs in $\Phi_k \setminus \Phi_k^{\text{NL}}$ form another point process denoted by Φ_k^{L} , representing the set of BSs with LoS path to the typical MU. As a consequence of the independence assumption of NLoS and LoS transmissions mentioned in the last paragraph, Φ_k^{NL} and Φ_k^{L} are two independent non-homogeneous PPPs with intensity functions $\lambda_k p_k^{\text{NL}}(\|\mathbf{X}_{k,i}\|)$ and $\lambda_k p_k^{\text{L}}(\|\mathbf{X}_{k,i}\|)$, respectively.

Based on assumptions above, the received power of the typical MU from a BS $\mathbf{X}_{k,i} \in \Phi_k$ is defined as follows.

Definition 1. The received power of the typical MU from a BS $\mathbf{X}_{k,i} \in \Phi_k$, *i.e.*, $P_{k,i}^{\text{rec}}$ is

$$P_{k,i}^{\text{rec}} = \begin{cases} P_k A_k^{\text{NL}} h_k^{\text{NL}} g_k^{\text{NL}} l_k^{\text{NL}}(\|\mathbf{X}_{k,i}\|), & \text{w. p. } p_k^{\text{NL}}(\|\mathbf{X}_{k,i}\|) \\ P_k A_k^{\text{L}} h_k^{\text{L}} g_k^{\text{L}} l_k^{\text{L}}(\|\mathbf{X}_{k,i}\|), & \text{w. p. } p_k^{\text{L}}(\|\mathbf{X}_{k,i}\|) \end{cases}, \quad (2)$$

where we denote $P_{k,i}^{\text{NL}} = P_k A_k^{\text{NL}} h_k^{\text{NL}} g_k^{\text{NL}} l_k^{\text{NL}}(\|\mathbf{X}_{k,i}\|)$, $P_{k,i}^{\text{L}} = P_k A_k^{\text{L}} h_k^{\text{L}} g_k^{\text{L}} l_k^{\text{L}}(\|\mathbf{X}_{k,i}\|)$, A_k^{NL} and A_k^{L} denote the respective path loss for NLoS and LoS transmissions at the reference distance (usually at 1 meter). For simplicity, denote $B_k^{\text{U}} = P_k A_k^{\text{U}}$ and let $l_k^{\text{U}}(\|\mathbf{X}_{k,i}\|) = \|\mathbf{X}_{k,i}\|^{-\alpha_k^{\text{U}}}$, where the superscript $\text{U} \in \{\text{NL}, \text{L}\} \stackrel{\text{def}}{=} \mathcal{U}$ used distinguishes NLoS and LoS transmissions and α_k^{U} denotes the path loss exponent for NLoS or LoS transmission in the k -th tier. Recently, [23] and [24] took bounded path loss model and stretched exponential path loss model into consideration, in which several interesting performance trends are found and will be investigated in our future work.

Remark 1. Apart from the fixed transmit power, a density-dependent transmit power is further assumed and analyzed mentioned in [25], *i.e.*, $P_k(\lambda) = \frac{10 \frac{T_k}{10} \eta}{A_k^{\text{NL}} r_k^{-\alpha_k^{\text{NL}}}}$, where $r_k = \sqrt{\frac{1}{\pi \lambda_k}}$ is the radius of an equivalent disk-shaped coverage area in the k -th tier with an area size of $r_k = \sqrt{\frac{1}{\pi}}$ and T_k is the per tier SINR threshold.

B. Cell Association Scheme

Cell association scheme [26] plays a crucial role in network performance determining BS coverage, MU hand-off regulation and even facility deployment of small cells. Conventionally, a typical MU is connected to the BS $\mathbf{X}_{k,m}$ if and only if

$$\mathcal{P}_{k,m}^{\text{dBm}} > \mathcal{P}_{j,n}^{\text{dBm}}, j \neq k, \quad (3)$$

where $\mathcal{P}_{k,m}^{\text{dBm}}$ is the instantaneous received power with dBm unit from the BS $\mathbf{X}_{k,m}$ and Eq. (3) is known as the MIRP association scheme.

In practical, $\mathcal{P}_k^{\text{dBm}}$ is usually averaged out in time and frequency domains to cope with fluctuations caused by channel

fading. In this text, a typical MU is connected to the BS $\mathbf{X}_{k,m}$ if and only if

$$\overline{\mathcal{P}}_{k,m}^{\text{dBm}} > \overline{\mathcal{P}}_{j,n}^{\text{dBm}}, j \neq k, \quad (4)$$

where $\overline{\mathcal{P}}_{k,m}^{\text{dBm}}$ denotes the average received power with dBm unit from the BS $\mathbf{X}_{k,m}$ and Eq. (4) is known as the MARP association scheme.

Aided by *cell range expansion* (CRE), which is realized by MUs adding a positive *cell range expansion bias* (CREB) to the received power from BSs in different tiers, more MUs can be offloaded to small cells. That is, if a MU is associated with the BS $\mathbf{X}_{k,m}$ if and only if

$$\overline{\mathcal{P}}_{k,m}^{\text{dBm}} + \Delta_{k,m}^{\text{dB}} > \overline{\mathcal{P}}_{j,n}^{\text{dBm}} + \Delta_{j,n}^{\text{dB}}, j \neq k, \quad (5)$$

where $\Delta_{k,m}^{\text{dB}}$ and $\Delta_{j,n}^{\text{dB}}$ is the CREB with dB unit in the k -th and j -th tier. With proper CREB chosen, the coverage of BSs in some tiers is artificially expanded, allowing MUs more flexible to be associated with BSs which may not provide the strongest received power, thus balancing traffic load to achieve spatial efficiency. However, CRE causes severe interference to small cell MU which impair the QoS of small cell users and thus *almost blank subframes* (ABS) coordination is needed between macrocell BSs and small cell BSs. However, the analysis of CRE plus ABS is challenging because (i) the association scheme is not only determined by the received power but also the current resource allocation strategy, and (ii) ignoring ABS while using CRE can impair the coverage performance. For simplicity, CRE and ABS are not going to be considered in this paper, which are left as our future work.

C. Performance Metrics

To evaluate the network performance, the following three metrics, *i.e.*, the coverage probability, the PT and the EE, are focused on.

The coverage probability is the probability that the received SINR is greater than a given threshold, *i.e.*, $p_{\text{cov}}(\{\lambda_k\}, \{T_k\}) = \Pr \left[\bigcup_{k \in \mathcal{K}, \mathbf{X}_{k,i} \in \Phi_k} \text{SINR}_k(\|\mathbf{X}_{k,i}\|) > T_k \right]$, where $\text{SINR}_k(\|\mathbf{X}_{k,i}\|)$ is defined as follows

$$\text{SINR}_k(\|\mathbf{X}_{k,i}\|) = \frac{P_k A_k^U h_k^U g_k^U l_k^U(\|\mathbf{X}_{k,i}\|)}{I_k + \eta}, \quad (6)$$

$$I_k = \sum_{k=1}^K \sum_{\mathbf{X}_{k,j} \in \Phi_k \setminus \mathbf{X}_{k,i}} P_k A_k^U h_k^U g_k^U l_k^U(\|\mathbf{X}_{k,j}\|), \quad (7)$$

where $\Phi_k \setminus \mathbf{X}_{k,i}$ is the Palm point process [27] representing the set of interfering BSs in the k -th tier and η denotes the noise power at the MU side, which is assumed to be the additive white Gaussian noise (AWGN).

The PT is defined as follows [24, 28]

$$\begin{aligned} \mathcal{T}(\{\lambda_k\}, \{T_k\}) &= \sum_{k=1}^K \lambda_k \mathcal{A}_k p_{\text{cov},k}^{\text{cond}} \log_2(1 + T_k) \\ &= \sum_{k=1}^K \lambda_k p_{\text{cov},k} \log_2(1 + T_k), \end{aligned} \quad (8)$$

where the network is fully loaded due to the assumption that $\lambda_u \gg \lambda_k$, \mathcal{A}_k is the association probability that the typical MU is connected to the k -th tier, $p_{\text{cov},k}^{\text{cond}}$ is the conditional association coverage probability and $p_{\text{cov},k}$ is the per-tier coverage probability. Compared with the area spectral efficiency (ASE), which is defined as

$$\begin{aligned} \text{ASE}(\{\lambda_k\}, \{T_k\}) &= \sum_{k=1}^K \mathbb{E}[\lambda_k \log_2(1 + \text{SINR}_k(\|\mathbf{X}_{k,i}\|))], \end{aligned} \quad (9)$$

the PT implicitly assumes a fixed rate transmission from all BSs in the network, and has a unit of bps/Hz/m², while the ASE assumes full buffers but it allows each link to adapt its rate to the optimal value for a given SINR, thus avoiding outages at low SINR and the wasting of rate at high SINR [24]. In other words, the PT is a more realistic performance metric and the ASE upper bounds the PT. In our analysis, the PT is chosen as our performance metric.

The EE is defined as the ratio between the PT and the total energy consumption of the network, *i.e.*,

$$\mathcal{E}(\{\lambda_k\}, \{T_k\}) = \frac{\mathcal{T}(\{\lambda_k\}, \{T_k\})}{\sum_{k=1}^K \lambda_k (a_k P_k + b_k)}, \quad (10)$$

where the coefficient a_k accounts for power consumption that scales with the average radiated power, and the term b_k models the static power consumed by signal processing, battery backup and cooling [29]. Other performance metrics, such as the bit-error probability and per-MU data rate, can be found using the coverage probability (SINR distribution) following the methods mentioned in [30].

III. PERFORMANCE ANALYSIS

In this section, we derive expressions for the considered performance metrics and study the effect of densification on these metrics. It is started by introducing the network transformation and then presenting the analytical expressions with the MIRP and MARP association schemes in the following subsections.

A. Network Transformation

Before presenting our main analytical results, firstly the network transformation is introduced, which aims to unify the analysis and to reduce the complexity as well.

Using the manipulation in [31, 32], we define

$$\overline{R}_{k,i}^{\text{NL}} = \|\mathbf{X}_{k,i}\| \cdot (B_k^{\text{NL}} g_k^{\text{NL}})^{-1/\alpha_k^{\text{NL}}}, \quad (11)$$

and

$$\overline{R}_{k,i}^{\text{L}} = \|\mathbf{X}_{k,i}\| \cdot (B_k^{\text{L}} g_k^{\text{L}})^{-1/\alpha_k^{\text{L}}}, \quad (12)$$

respectively. Then Eq. (2) can be written as

$$P_{k,i}^{\text{rec}} = \begin{cases} P_{k,i}^{\text{NL}} = h_k^{\text{NL}} \left(\overline{R}_{k,i}^{\text{NL}} \right)^{-\alpha_k^{\text{NL}}}, & \text{w. p. } p_k^{\text{NL}}(\|\mathbf{X}_{k,i}\|) \\ P_{k,i}^{\text{L}} = h_k^{\text{L}} \left(\overline{R}_{k,i}^{\text{L}} \right)^{-\alpha_k^{\text{L}}}, & \text{w. p. } p_k^{\text{L}}(\|\mathbf{X}_{k,i}\|) \end{cases}. \quad (13)$$

By adopting the Equivalence Theorem in [31], it is concluded that the distance $\{\overline{R_{k,i}^{\text{NL}}}\}_i$ (or $\{\overline{R_{k,i}^{\text{L}}}\}_i$) from a scaled point process for NLoS BSs (or LoS BSs), which still remains a PPP denoted by $\overline{\Phi_k^{\text{NL}}}$ (or $\overline{\Phi_k^{\text{L}}}$). $\{\overline{\Phi_k^{\text{U}}}\}_k, \mathbf{U} \in \mathcal{U}$ are mutually independent with each other, and the intensity measures and intensities are provided in Lemma 1 as below.

Lemma 1. The intensity measure and intensity of $\overline{\Phi_k^{\text{U}}}$ can be formulated as

$$\lambda_k^{\text{NL}}(t) = \frac{d}{dt} \Lambda_k^{\text{NL}}([0, t]), \quad (14)$$

and

$$\lambda_k^{\text{L}}(t) = \frac{d}{dt} \Lambda_k^{\text{L}}([0, t]), \quad (15)$$

respectively, where

$$\Lambda_k^{\text{NL}}([0, t]) = \mathbb{E}_{g_k^{\text{NL}}} \left[2\pi \lambda_k \int_{z=0}^{t(B_k^{\text{NL}} g_k^{\text{NL}})^{1/\alpha_k^{\text{NL}}}} p_k^{\text{NL}}(z) z dz \right] \quad (16)$$

and

$$\Lambda_k^{\text{L}}([0, t]) = \mathbb{E}_{g_k^{\text{L}}} \left[2\pi \lambda_k \int_{z=0}^{t(B_k^{\text{L}} g_k^{\text{L}})^{1/\alpha_k^{\text{L}}}} p_k^{\text{L}}(z) z dz \right]. \quad (17)$$

Proof: The proof can be referred to [31, Appendix A] and thus omitted here. Aided by the network transformation and stochastic geometry tool, the coverage probability, the PT and the EE will be derived in the following. ■

B. Coverage Probability with the MIRP Association Scheme

With the MIRP association scheme, the typical MU is associated with the BS which offers the maximum instantaneous received power as shown in Eq. (3). Using this cell association scheme and considering Lemma 1, the general results of coverage probability in the K -tier HetNets is given by Theorem 1.

Theorem 1. When $T_k \geq 1$, the coverage probability for a typical MU with the MIRP association scheme can be derived as

$$\begin{aligned} p_{\text{cov}}^{\text{MIRP}}(\{\lambda_k\}, \{T_k\}) &= \sum_{k=1}^K \int_{r=0}^{\infty} \lambda_k^{\text{NL}}(r) e^{-T_k \eta r^{\alpha_k^{\text{NL}}}} \\ &\times \prod_{j=1}^K [\mathcal{L}_{I_j^{\text{NL}}}^{\text{MIRP}}(T_k r^{\alpha_k^{\text{NL}}}) \mathcal{L}_{I_j^{\text{L}}}^{\text{MIRP}}(T_k r^{\alpha_k^{\text{NL}}})] dr \\ &+ \sum_{k=1}^K \lambda_k^{\text{L}}(r) \int_{t=0}^{\infty} e^{-T_k \eta r^{\alpha_k^{\text{L}}}} \\ &\times \prod_{j=1}^K [\mathcal{L}_{I_j^{\text{NL}}}^{\text{MIRP}}(T_k r^{\alpha_k^{\text{L}}}) \mathcal{L}_{I_j^{\text{L}}}^{\text{MIRP}}(T_k r^{\alpha_k^{\text{L}}})] dr, \end{aligned} \quad (18)$$

where

$$\mathcal{L}_{I_j^{\text{NL}}}^{\text{MIRP}}(s) = \exp \left[- \int_{y=0}^{\infty} \frac{\lambda_j^{\text{NL}}(y)}{1 + y^{\alpha_j^{\text{NL}}}/s} dy \right], \quad (19)$$

and

$$\mathcal{L}_{I_j^{\text{L}}}^{\text{MIRP}}(s) = \exp \left[- \int_{y=0}^{\infty} \frac{\lambda_j^{\text{L}}(y)}{1 + y^{\alpha_j^{\text{L}}}/s} dy \right]. \quad (20)$$

Proof: See Appendix A. ■

In pursuit of the analytical results of the PT and the EE, the NLoS/LoS coverage probability and per-tier coverage probability are presented in the following two corollaries.

Corollary 1. When $T_k \geq 1$, the coverage probability for a typical MU which is served by NLoS BSs and LoS BSs with the MIRP association scheme are given by

$$\begin{aligned} p_{\text{cov,NL}}^{\text{MIRP}}(\{\lambda_k\}, \{T_k\}) &= \sum_{k=1}^K p_{\text{NL},k}^{\text{MIRP}}(\{\lambda_k\}, \{T_k\}) \\ &= \sum_{k=1}^K \int_{r=0}^{\infty} \lambda_k^{\text{NL}}(r) e^{-T_k \eta r^{\alpha_k^{\text{NL}}}} \\ &\times \prod_{j=1}^K [\mathcal{L}_{I_j^{\text{NL}}}^{\text{MIRP}}(T_k r^{\alpha_k^{\text{NL}}}) \mathcal{L}_{I_j^{\text{L}}}^{\text{MIRP}}(T_k r^{\alpha_k^{\text{NL}}})] dr, \end{aligned} \quad (21)$$

and

$$\begin{aligned} p_{\text{cov,L}}^{\text{MIRP}}(\{\lambda_k\}, \{T_k\}) &= \sum_{k=1}^K p_{\text{L},k}^{\text{MIRP}}(\{\lambda_k\}, \{T_k\}) \\ &= \sum_{k=1}^K \int_{t=0}^{\infty} \lambda_k^{\text{L}}(r) e^{-T_k \eta r^{\alpha_k^{\text{L}}}} \\ &\times \prod_{j=1}^K [\mathcal{L}_{I_j^{\text{NL}}}^{\text{MIRP}}(T_k r^{\alpha_k^{\text{L}}}) \mathcal{L}_{I_j^{\text{L}}}^{\text{MIRP}}(T_k r^{\alpha_k^{\text{L}}})] dr, \end{aligned} \quad (22)$$

respectively.

Proof: This corollary can be derived from Theorem 1 by rearranging the terms in Eq. (18) and thus the proof is omitted here. ■

Corollary 2. When $T_k \geq 1$, the per-tier coverage probability for a typical MU which is covered by the k -th tier with the MIRP association scheme is given by

$$\begin{aligned} p_{\text{cov},k}^{\text{MIRP}}(\{\lambda_k\}, \{T_k\}) &= \int_{r=0}^{\infty} \lambda_k^{\text{NL}}(r) e^{-T_k \eta r^{\alpha_k^{\text{NL}}}} \\ &\times \prod_{j=1}^K [\mathcal{L}_{I_j^{\text{NL}}}^{\text{MIRP}}(T_k r^{\alpha_k^{\text{NL}}}) \mathcal{L}_{I_j^{\text{L}}}^{\text{MIRP}}(T_k r^{\alpha_k^{\text{NL}}})] dr \\ &+ \int_{t=0}^{\infty} \lambda_k^{\text{L}}(r) e^{-T_k \eta r^{\alpha_k^{\text{L}}}} \\ &\times \prod_{j=1}^K [\mathcal{L}_{I_j^{\text{NL}}}^{\text{MIRP}}(T_k r^{\alpha_k^{\text{L}}}) \mathcal{L}_{I_j^{\text{L}}}^{\text{MIRP}}(T_k r^{\alpha_k^{\text{L}}})] dr. \end{aligned} \quad (23)$$

Proof: This corollary can be derived from Theorem 1 by rearranging the terms in Eq. (18) and thus the proof is omitted here. ■

C. Coverage Probability with the MARP Association Scheme

With the MARP association scheme, the typical MU is associated with the BS which offers the maximum long-term averaged received power by averaging out the effect of multi-path fading h_k^{U} . With this cell association scheme, the primary results of coverage probability is given by Theorem 2. ■

Theorem 2. The coverage probability for a typical MU with the MARP association scheme is

$$\begin{aligned}
 p_{\text{cov}}^{\text{MARP}}(\{\lambda_k\}, \{T_k\}) &= \sum_{k=1}^K p_{k,\text{NL}}^{\text{MARP}}(\{\lambda_k\}, \{T_k\}) \\
 &+ \sum_{k=1}^K p_{k,\text{L}}^{\text{MARP}}(\{\lambda_k\}, \{T_k\}) \\
 &= \sum_{k=1}^K \int_{r=0}^{\infty} \lambda_k^{\text{NL}}(r) \prod_{j=1}^K [\mathcal{L}_{I_j^{\text{NL}}}^{\text{MARP1}}(T_k r^{\alpha_k^{\text{NL}}}) \mathcal{L}_{I_j^{\text{L}}}^{\text{MARP1}}(T_k r^{\alpha_k^{\text{NL}}})] \\
 &\times e^{-\sum_{j=1}^K [\Lambda_j^{\text{L}}([0, r^{\alpha_k^{\text{NL}}/\alpha_j^{\text{L}}})] + \Lambda_j^{\text{NL}}([0, r^{\alpha_k^{\text{NL}}/\alpha_j^{\text{NL}}})]} - T_k \eta r^{\alpha_k^{\text{NL}}} dr \\
 &+ \sum_{k=1}^K \int_{r=0}^{\infty} \lambda_k^{\text{L}}(r) \prod_{j=1}^K [\mathcal{L}_{I_j^{\text{NL}}}^{\text{MARP2}}(T_k r^{\alpha_k^{\text{L}}}) \mathcal{L}_{I_j^{\text{L}}}^{\text{MARP2}}(T_k r^{\alpha_k^{\text{L}}})] \\
 &\times e^{-\sum_{j=1}^K [\Lambda_j^{\text{L}}([0, r^{\alpha_k^{\text{L}}/\alpha_j^{\text{L}}})] + \Lambda_j^{\text{NL}}([0, r^{\alpha_k^{\text{L}}/\alpha_j^{\text{NL}}})]} - T_k \eta r^{\alpha_k^{\text{L}}} dr, \quad (24)
 \end{aligned}$$

where

$$\mathcal{L}_{I_j^{\text{NL}}}^{\text{MARP1}}(s) = \exp\left[-\int_{y=r^{\alpha_k^{\text{NL}}/\alpha_j^{\text{NL}}}}^{\infty} \frac{\lambda_j^{\text{NL}}(y)}{1+y^{\alpha_j^{\text{NL}}/s}} dy\right], \quad (25)$$

$$\mathcal{L}_{I_j^{\text{L}}}^{\text{MARP1}}(s) = \exp\left[-\int_{y=r^{\alpha_k^{\text{L}}/\alpha_j^{\text{L}}}}^{\infty} \frac{\lambda_j^{\text{L}}(y)}{1+y^{\alpha_j^{\text{L}}/s}} dy\right], \quad (26)$$

$$\mathcal{L}_{I_j^{\text{NL}}}^{\text{MARP2}}(s) = \exp\left[-\int_{y=r^{\alpha_k^{\text{L}}/\alpha_j^{\text{NL}}}}^{\infty} \frac{\lambda_j^{\text{NL}}(y)}{1+y^{\alpha_j^{\text{NL}}/s}} dy\right], \quad (27)$$

and

$$\mathcal{L}_{I_j^{\text{L}}}^{\text{MARP2}}(s) = \exp\left[-\int_{y=r^{\alpha_k^{\text{L}}/\alpha_j^{\text{L}}}}^{\infty} \frac{\lambda_j^{\text{L}}(y)}{1+y^{\alpha_j^{\text{L}}/s}} dy\right]. \quad (28)$$

Proof: See Appendix B. ■

Remark 2. Note that different from Theorem 1, Theorem 2 can be applied to scenarios without the assumption of a particular range of SINR threshold T_k , e.g., $T_k \geq 1$.

Similar to the study for Theorem 1, we provide two corollaries, i.e., the NLoS/LoS coverage probability and the per-tier coverage probability, as follows.

Corollary 3. The coverage probability for a typical MU which is served by NLoS BSs and LoS BSs with the MARP association scheme are given by

$$\begin{aligned}
 p_{\text{cov,NL}}^{\text{MARP}}(\{\lambda_k\}, \{T_k\}) &= \sum_{k=1}^K p_{\text{NL},k}^{\text{MARP}}(\{\lambda_k\}, \{T_k\}) \\
 &= \sum_{k=1}^K \int_{r=0}^{\infty} \lambda_k^{\text{NL}}(r) \prod_{j=1}^K [\mathcal{L}_{I_j^{\text{NL}}}^{\text{MARP1}}(T_k r^{\alpha_k^{\text{NL}}}) \mathcal{L}_{I_j^{\text{L}}}^{\text{MARP1}}(T_k r^{\alpha_k^{\text{NL}}})] \\
 &\times e^{-\sum_{j=1}^K [\Lambda_j^{\text{L}}([0, r^{\alpha_k^{\text{NL}}/\alpha_j^{\text{L}}})] + \Lambda_j^{\text{NL}}([0, r^{\alpha_k^{\text{NL}}/\alpha_j^{\text{NL}}})]} - T_k \eta r^{\alpha_k^{\text{NL}}} dr \quad (29)
 \end{aligned}$$

and

$$\begin{aligned}
 p_{\text{cov,L}}^{\text{MARP}}(\{\lambda_k\}, \{T_k\}) &= \sum_{k=1}^K p_{\text{L},k}^{\text{MARP}}(\{\lambda_k\}, \{T_k\}) \\
 &= \sum_{k=1}^K \int_{r=0}^{\infty} \lambda_k^{\text{L}}(r) \prod_{j=1}^K [\mathcal{L}_{I_j^{\text{NL}}}^{\text{MARP2}}(T_k r^{\alpha_k^{\text{L}}}) \mathcal{L}_{I_j^{\text{L}}}^{\text{MARP2}}(T_k r^{\alpha_k^{\text{L}}})] \\
 &\times e^{-\sum_{j=1}^K [\Lambda_j^{\text{L}}([0, r^{\alpha_k^{\text{L}}/\alpha_j^{\text{L}}})] + \Lambda_j^{\text{NL}}([0, r^{\alpha_k^{\text{L}}/\alpha_j^{\text{NL}}})]} - T_k \eta r^{\alpha_k^{\text{L}}} dr, \quad (30)
 \end{aligned}$$

respectively.

Proof: This corollary can be derived from Theorem 2 by rearranging the terms in Eq. (24) and thus the proof is omitted here. ■

Corollary 4. The per-tier coverage probability for a typical MU which is covered by the k -th tier with the MARP association scheme is given by

$$\begin{aligned}
 p_{\text{cov},k}^{\text{MARP}}(\{\lambda_k\}, \{T_k\}) &= \int_{r=0}^{\infty} \lambda_k^{\text{NL}}(r) e^{-T_k \eta r^{\alpha_k^{\text{NL}}}} \\
 &\times \prod_{j=1}^K [\mathcal{L}_{I_j^{\text{NL}}}^{\text{MARP1}}(T_k r^{\alpha_k^{\text{NL}}}) \mathcal{L}_{I_j^{\text{L}}}^{\text{MARP1}}(T_k r^{\alpha_k^{\text{NL}}})] \\
 &\times e^{-\sum_{j=1}^K [\Lambda_j^{\text{L}}([0, r^{\alpha_k^{\text{NL}}/\alpha_j^{\text{L}}})] + \Lambda_j^{\text{NL}}([0, r^{\alpha_k^{\text{NL}}/\alpha_j^{\text{NL}}})]} dr \\
 &+ \int_{r=0}^{\infty} \lambda_k^{\text{L}}(r) \prod_{j=1}^K [\mathcal{L}_{I_j^{\text{NL}}}^{\text{MARP2}}(T_k r^{\alpha_k^{\text{L}}}) \mathcal{L}_{I_j^{\text{L}}}^{\text{MARP2}}(T_k r^{\alpha_k^{\text{L}}})] \\
 &\times e^{-\sum_{j=1}^K [\Lambda_j^{\text{L}}([0, r^{\alpha_k^{\text{L}}/\alpha_j^{\text{L}}})] + \Lambda_j^{\text{NL}}([0, r^{\alpha_k^{\text{L}}/\alpha_j^{\text{NL}}})]} - T_k \eta r^{\alpha_k^{\text{L}}} dr. \quad (31)
 \end{aligned}$$

Proof: This corollary can be derived from Theorem 2 by rearranging the terms in Eq. (24) and thus the proof is omitted here. ■

Intuitively, the coverage probability with the MIRP association scheme is higher than that with the MARP association scheme. However, it can be proved mathematically which is summarized in the following corollary.

Corollary 5. In the studied K -tier HetNet, the coverage probability with the MIRP association scheme is higher than that with the MARP association scheme, where the gap is determined by the intensity and the intensity measure.

Proof: See Appendix C. ■

D. The PT and the EE

As the results with the MIRP and the MARP association schemes are some kind of similar and the MARP association scheme is more practical in the real network, we take the MARP association scheme as an example to evaluate the PT and the EE in the following. The PT with the MARP association scheme can be directly obtained from the coverage probability expressions using Eq. (8), i.e.,

$$\mathcal{T}(\{\lambda_k\}, \{T_k\}) = \sum_{k=1}^K \lambda_k p_{\text{cov},k}^{\text{MARP}}(\{\lambda_k\}, \{T_k\}) \log_2(1 + T_k). \quad (32)$$

While the PT with the MIRP association scheme is similar except for replacing $p_{\text{cov},k}^{\text{MARP}}(\{\lambda_k\}, \{T_k\})$ by $p_{\text{cov},k}^{\text{MIRP}}(\{\lambda_k\}, \{T_k\})$.

The EE can be derived by using Eq. (10) and we will only provide expressions for it when necessary.

IV. PERFORMANCE OPTIMIZATION AND TRADEOFF

As mentioned, from the mobile operators' point of view, the commercial viability of network densification depends on the underlying capital and operational expenditure [9]. While the former cost may be covered by taking up a high volume of customers, with the rapid rise in the price of energy, and given that BSs are particularly power-hungry, EE has become an increasingly crucial factor for the success of dense HetNets [10]. There are two main approaches to enhance the energy consumption of cellular networks: 1) improvement in hardware and 2) energy-efficient system design. The improvement in hardware may have achieved its bottleneck due to the limit of Moore's law, while the energy-efficient system design has a great potential in the future 5G networks. In the following, two energy-efficient optimization problems are proposed trying to obtain insights of the system design.

A. Optimizing coverage probability with the maximum total power consumption constraint

To pursue a further study on coverage performance, we formulate a theoretical framework which determines the optimal BS density to maximize the coverage probability while guaranteeing that the total area power consumption is lower than a given expected value P^{max} as follows

$$\begin{aligned} \text{OP1} : & \max_{\lambda_k} p_{\text{cov}}^{\text{MARP}}(\{\lambda_k\}, \{T_k\}) \\ \text{s. t. C1:} & \sum_{k=1}^K \lambda_k (a_k P_k + b_k) \leq P^{\text{max}} \\ \text{C2:} & \lambda_k \geq 0, \forall k \in \mathcal{K} \end{aligned} \quad (33)$$

where a_k and b_k are defined in Eq. (10). Note that **OP1** assumes the MARP association scheme, while the optimization problem with the MIRP association scheme is similar to **OP1** and omitted here for brevity.

B. Optimizing the EE under the minimum coverage probability constraint

In this subsection, another framework are formulated which determines the optimal BS density to maximize the EE while guaranteeing QoS of the network, *i.e.*, the coverage probability is higher than a given expected value $p_{\text{cov}}^{\text{min}}$ as follows

$$\begin{aligned} \text{OP2} : & \max_{\lambda_k} \mathcal{E}(\{\lambda_k\}, \{T_k\}) \\ \text{s. t. C1:} & p_{\text{cov}}^{\text{MARP}}(\{\lambda_k\}, \{T_k\}) \geq p_{\text{cov}}^{\text{min}} \\ \text{C2:} & \lambda_k \geq 0, \forall k \in \mathcal{K} \end{aligned} \quad (34)$$

We will show in the simulation results that tradeoff exists between the coverage probability and the EE.

C. Optimal deployment solution

As NLoS and LoS transmissions are incorporated into our model, the coverage probability is not a monotonically increasing function with respect to BS density λ_k like the cases in [10, 29, 33, 34] anymore. Besides, the coverage probability function is not convex with respect to λ_k , either. Therefore, the optimization problem under consideration should be tackled numerically. Exhaustive search algorithms are well-suited for tackling the problem considering that the objective function derivative is not available analytically and its accurate evaluation is resource-intensive. Brent's algorithm [35] and heuristic downhill simplex method [36] can be utilized to obtain the solutions of **OP1** and **OP2** in exponential time. To gain an analytical insight into the effect of different operational settings on the maximum energy-efficient deployment solution, in the following, we focus on the problem of finding the optimal BS density in a 2-tier HetNet.

V. RESULTS AND INSIGHTS

A 2-tier HetNet is considered in our analysis. Macrocell BSs are in Tier 1 and small cell BSs are in Tier 2. We assume that $P_1 = 46$ dBm, $P_2 = 24$ dBm, $A_1^{\text{NL}} = 2.7$, $A_1^{\text{L}} = 30.8$, $A_2^{\text{NL}} = 32.9$, $A_2^{\text{L}} = 41.1$, $\alpha_1^{\text{NL}} = 4.28$, $\alpha_1^{\text{L}} = 2.42$, $\alpha_2^{\text{NL}} = 3.75$, $\alpha_2^{\text{L}} = 2.09$, $\sigma_1^{\text{NL}} = 8$ dB, $\sigma_1^{\text{L}} = 4$ dB, $\sigma_2^{\text{NL}} = 4$ dB, $\sigma_2^{\text{L}} = 3$ dB, $\eta = -95$ dBm [18, 19, 31, 37–41] unless stated otherwise.

A. Validation of the Analytical Results of Coverage Probability with Monte Carlo Simulations

If fixing λ_2 , the analytical and simulation results of $p_{\text{cov}}^{\text{MIRP}}(\{\lambda_k\}, \{T_k\})$ and the analytical results of $p_{\text{cov}}^{\text{MARP}}(\{\lambda_k\}, \{T_k\})$ configured with $T = 1$ dB are plotted in Fig. 1 and Fig. 2, respectively. As can be observed from Fig. 1, the analytical results match the simulation results well, which validate the accuracy of our theoretical analysis. In Fig. 2, aided by the utilization of a density-dependent BS transmit power, the coverage probability improves a lot as λ_1 increases.

Fig. 3 and Fig. 4 illustrate the coverage probability vs. the ratio of λ_1 and λ_2 , *i.e.*, $\frac{\lambda_1}{\lambda_2}$ with the MIRP association scheme and the MIRP association scheme when λ_1 (or λ_2) is fixed. It is found that in Fig. 3, there is always a coverage peak when $\frac{\lambda_1}{\lambda_2}$ is low, medium and high, *i.e.*, $p_{\text{cov}}^{\text{max}} = 0.3417$ (or 0.3725 with the MIRP), $p_{\text{cov}}^{\text{max}} = 0.6998$ (or 0.7868 with the MIRP), $p_{\text{cov}}^{\text{max}} = 0.6521$ (or 0.7476 with the MIRP), which indicates that there exists an optimal λ_1 when implementing the network design if λ_2 is fixed. And in Fig. 4, the optimal λ_2 exists as well. However, compared with Fig. 3, when the fixed value of λ_1 is sparse, the coverage probability firstly increases and then reaches a peak. Finally it decreases to a certain value. When the fixed value of λ_1 becomes larger, the coverage probability saturates. Based on the above observations, dense deployment of small cell BSs and macrocell BSs will lead to a better coverage probability. However, there is no need to deploy an infinite number of BSs in a finite area. When λ_1 approaches infinite if λ_2 remains fixed, and vice versa, the coverage probability becomes much worse. In contrast, when

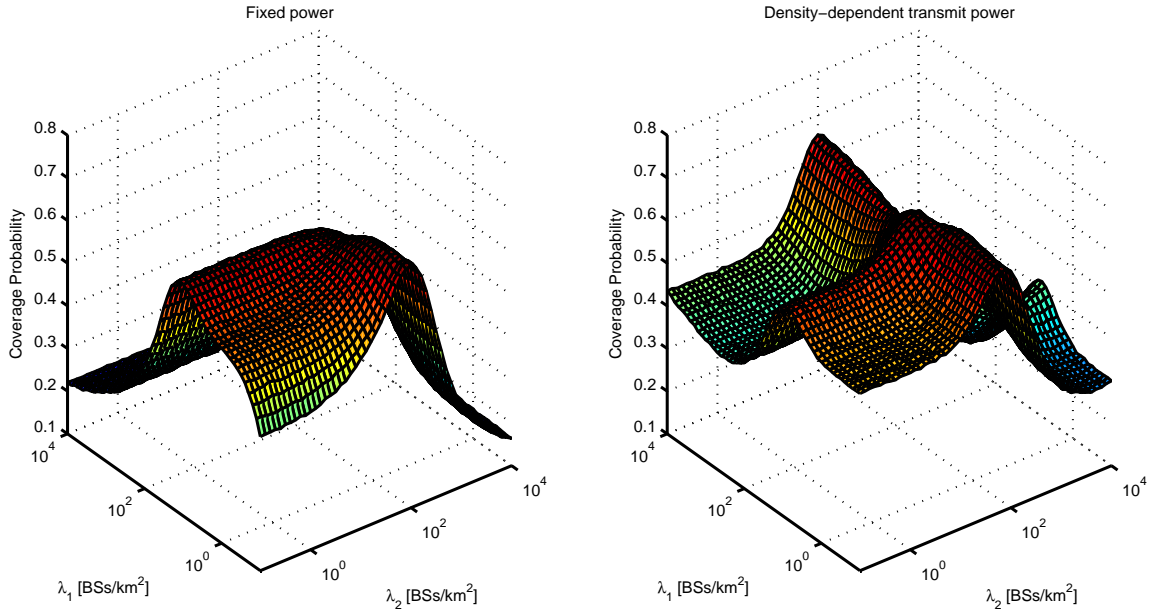


Figure 6. Comparison of coverage probability based on different transmit power models, *i.e.*, the fixed transmit power and density-dependent transmit power.

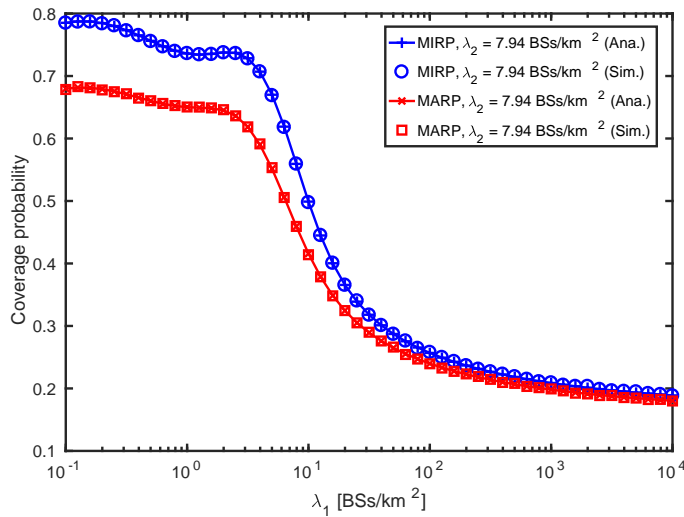


Figure 1. Coverage probability vs. λ_1 with the MIRP and MARP association schemes, $T_k = 1$ dB.

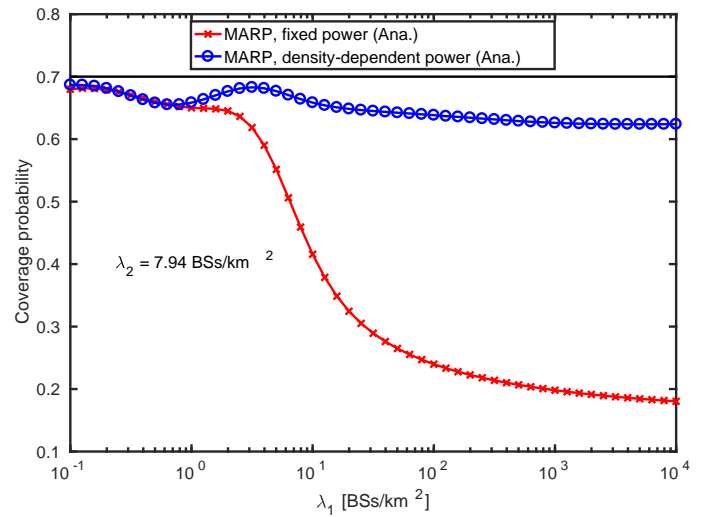


Figure 2. Coverage probability vs. λ_1 with the MARP association scheme, $T_k = 1$ dB.

λ_1 goes to zero if λ_2 is fixed, and vice versa, the coverage probability saturates to a certain value.

To have a full picture of the coverage probability with respect to λ_1 and λ_2 , present two 3D figures are presented in Fig. 5 and Fig. 6. In Fig. 5, we compare the MIRP and MARP association schemes based on the fixed transmit power. It is found that the coverage probability with the MIRP association scheme is always greater than that with the MARP association scheme as with former association scheme BSs can provide the maximum power all the time even though it is not practical in the real networks. In Fig. 6, coverage probability based on the fixed transmit power and density-dependent transmit power are illustrated, respectively. By utilizing a density-dependent

transmit power, the coverage probability improves compared with the HetNets using a fixed transmit power. Besides, it is noted that the coverage probability using a density-dependent transmit power fluctuates with BS density as illustrated in Fig. 6 as well as in Fig. 2. It is because the imperfect power control used in Remark 1 which only depends on BS densities and an approximate equivalent coverage area, the 3D coverage probability appears more unique than that using a fixed transmit power.

B. The PT and the EE

In this subsection, two typical energy consumption scenarios are considered, *i.e.*, practical power consumption and ideal

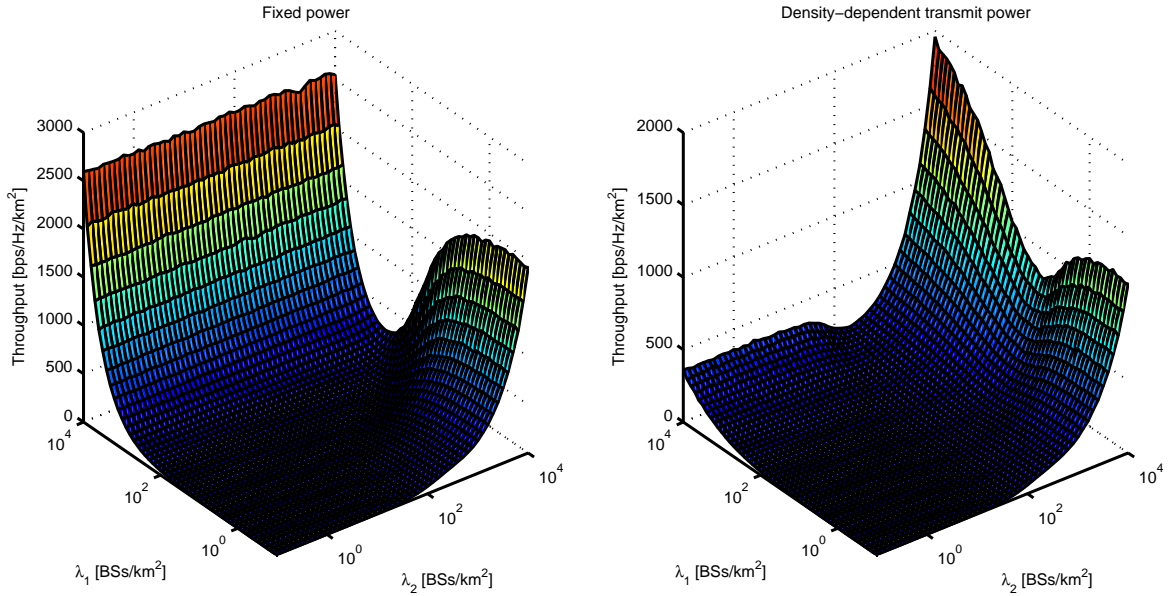


Figure 7. The PT vs. λ_1 and λ_2 based on the fixed transmit power and density-dependent transmit power.

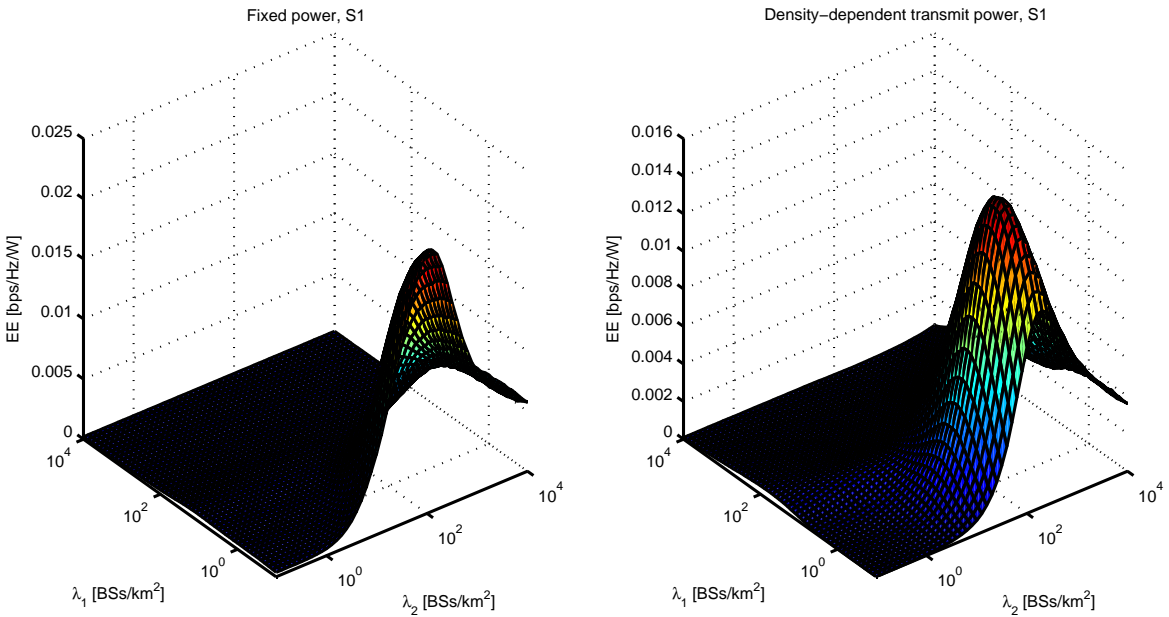


Figure 8. The EE vs. λ_1 and λ_2 based on the fixed transmit power and density-dependent transmit power in scenario S1.

power consumption, denoted by **S1** and **S2**. Recall that the definition of the EE in Eq. (10) have parameters $\{a_k\}$ and $\{b_k\}$, thus we define **S1** as the HetNets which are configured with $\{a_1 = 22.6, a_2 = 5.5, b_1 = 414.2, b_2 = 32\}$ [29] and **S2** configured with $\{a_1 = 1, a_2 = 1, b_1 = 0, b_2 = 0\}$, respectively. Note that **S2** accounts for the HetNets with perfect power amplifier and ignoring the static power consumed by signal processing, battery backup, and cooling, *etc.* In other words, in **S2** only radiated power is considered. It is observed that λ_1 has a greater impact on the PT than λ_2 in Fig. 7.

However, a larger λ_1 can not always provide a better EE as illustrated in Fig. 8 and Fig. 9. Therefore, there should exist a tradeoff among coverage probability, the PT and the EE, which is revealed in the following subsection.

C. Optimal Deployment Solutions

In this subsection, present the optimal deployment solutions for **OP1** and **OP2** are presented. Regarding **OP1**, Fig. 10, Fig. 11 and Fig. 12 offer the optimal coverage probability, the optimal λ_2 and the optimal λ_1 with respect to P^{\max} ,

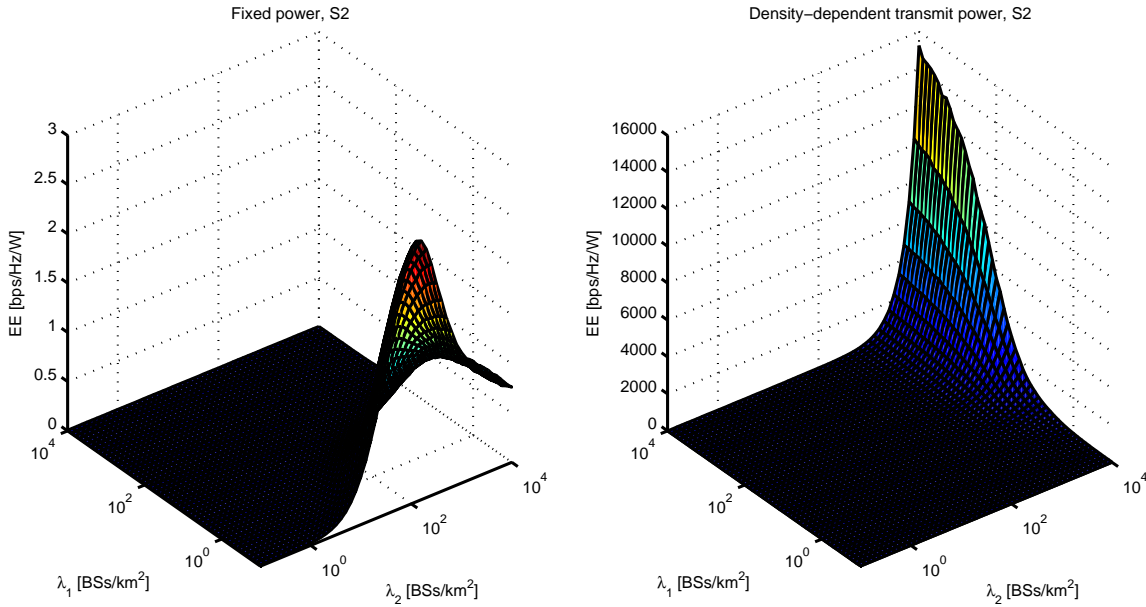


Figure 9. The EE vs. λ_1 and λ_2 based on the fixed transmit power and density-dependent transmit power in scenario **S2**.

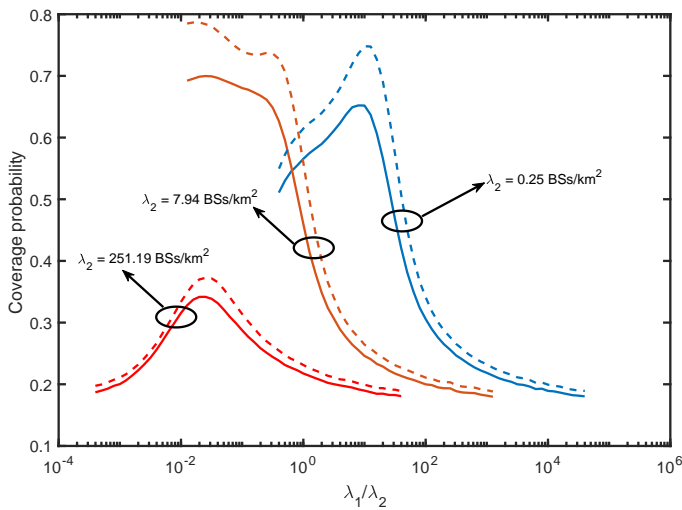


Figure 3. Coverage probability vs. $\frac{\lambda_1}{\lambda_2}$ with the MARP association scheme (the solid line) and the MIRP association scheme (the dashed line) when λ_2 is fixed, $T_k = 1$ dB.

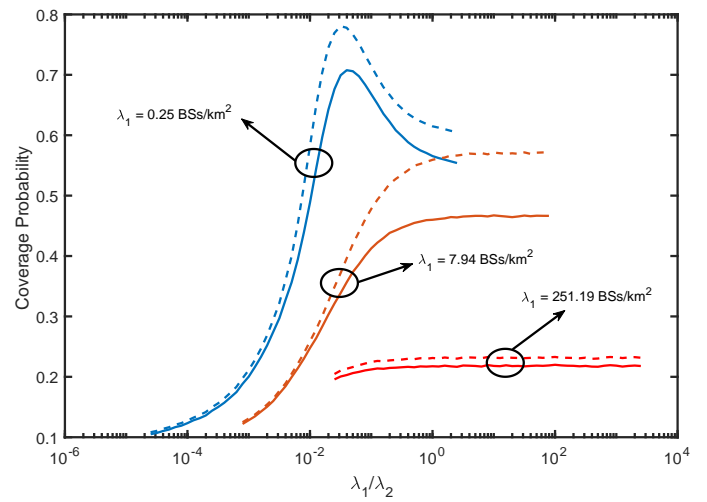


Figure 4. Coverage probability vs. $\frac{\lambda_1}{\lambda_2}$ with the MARP association scheme (the solid line) and the MIRP association scheme (the dashed line) when λ_1 is fixed, $T_k = 1$ dB.

respectively. From Fig. 10, we conclude that the maximum coverage probability increases with the increase of P^{\max} and finally becomes invariant with P^{\max} . The reason behind this is that a larger P^{\max} provides more flexible BS deployment choice which will finally approach the optimal BS deployment without the constraint of power consumption. Besides, the maximum coverage probability of HetNets with a density-dependent transmit power is more sensitive than that with a fixed transmit power. By comparison, the maximum coverage probability in **S2** is superior to that in **S1** when P^{\max} is small and inferior to that in **S1** when P^{\max} becomes large. The optimal λ_2 in **S1** grows up to a certain value with the increase of P^{\max} , after which the optimal λ_2 reaches its saturation,

as illustrated in Fig. 11. While in **S2**, the optimal λ_2 has an opposite tendency compared with that in **S1**. It is because, in **S1**, static power consumption takes up most of the total power, especially for the macrocell BSs. Therefore, deploying more small cell BSs can save much more energy. If ignoring the static power consumption, *i.e.*, **S2** is considered, every single macrocell BS can provide a better coverage performance than every single small cell BS, thus more macrocell BSs should be deployed in this scenario as shown in Fig. 12.

Regarding **OP2**, Fig. 13, Fig. 14 and Fig. 15 present the maximum EE, the optimal λ_2 and λ_1 , respectively. It is observed in Fig. 13 that the maximum EE is a decreasing function with respect to p_{cov}^{\min} . It is because a smaller p_{cov}^{\min}

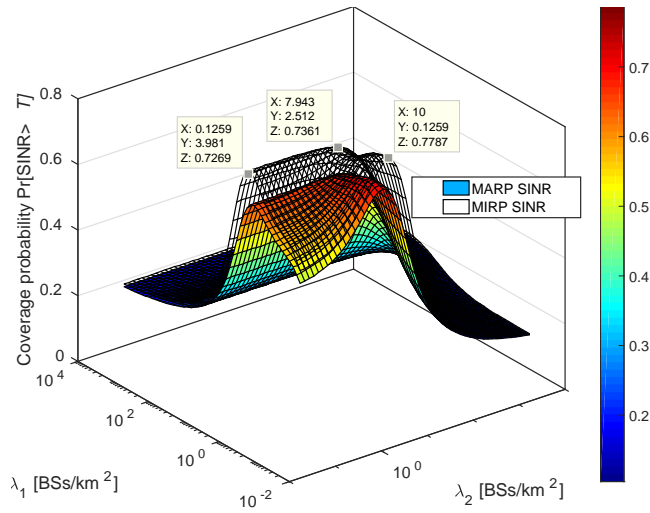


Figure 5. Comparison of coverage probability with the MIRP and MARP association schemes.

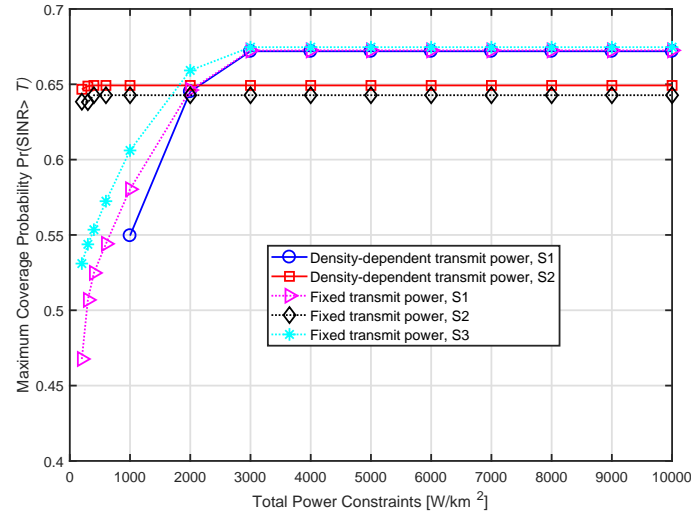


Figure 10. OP1: The Maximum coverage probability vs. P^{\max} in scenarios S1, S2 and S3 ($S3: \{a_1 = 10.3, a_2 = 5.5, b_1 = 156.2, b_2 = 32\}$).

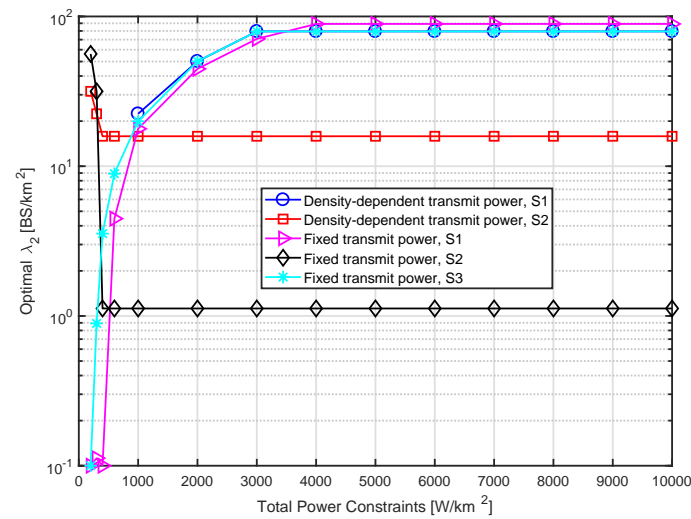


Figure 11. OP1: The optimal λ_2 vs. P^{\max} in scenarios S1, S2 and S3 ($S3: \{a_1 = 10.3, a_2 = 5.5, b_1 = 156.2, b_2 = 32\}$).

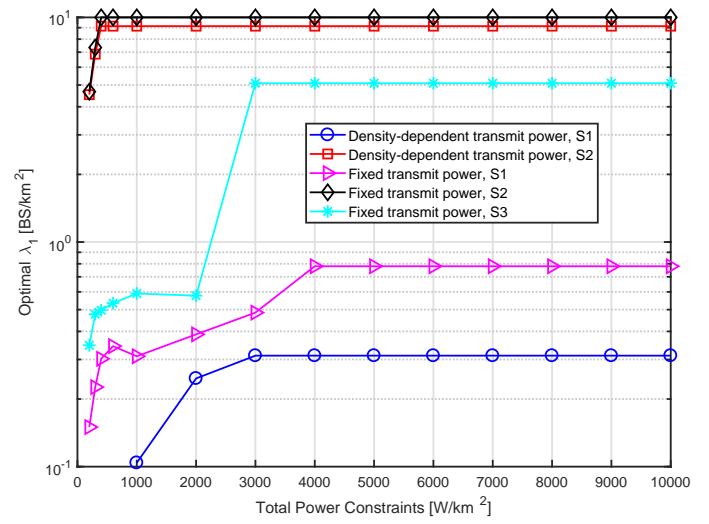


Figure 12. OP1: The optimal λ_1 vs. P^{\max} in scenarios S1, S2 and S3 ($S3: \{a_1 = 10.3, a_2 = 5.5, b_1 = 156.2, b_2 = 32\}$).

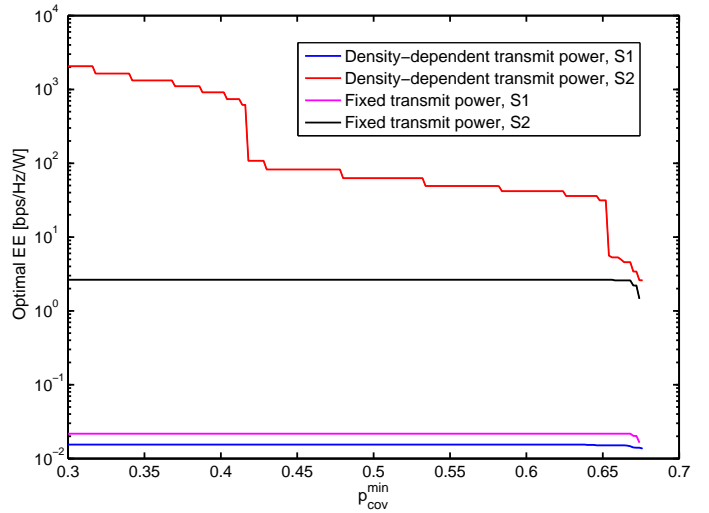


Figure 13. OP2: The maximum EE vs. p_{cov}^{\min} in scenarios S1 and S2.

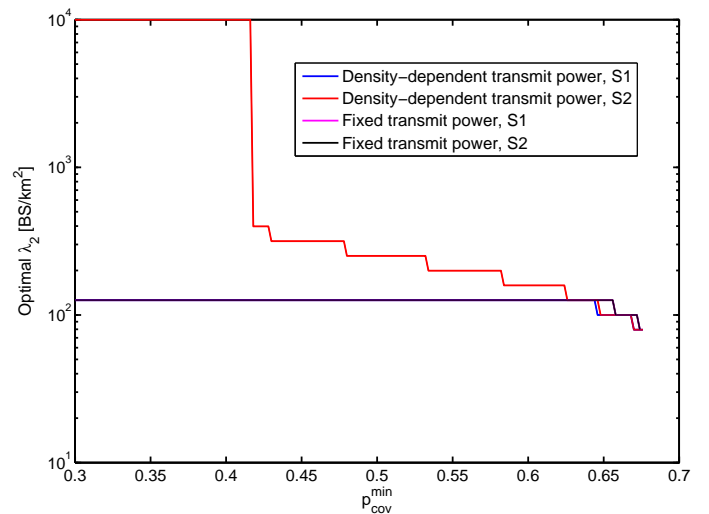


Figure 14. OP2: The optimal λ_2 vs. p_{cov}^{\min} in scenarios S1 and S2.

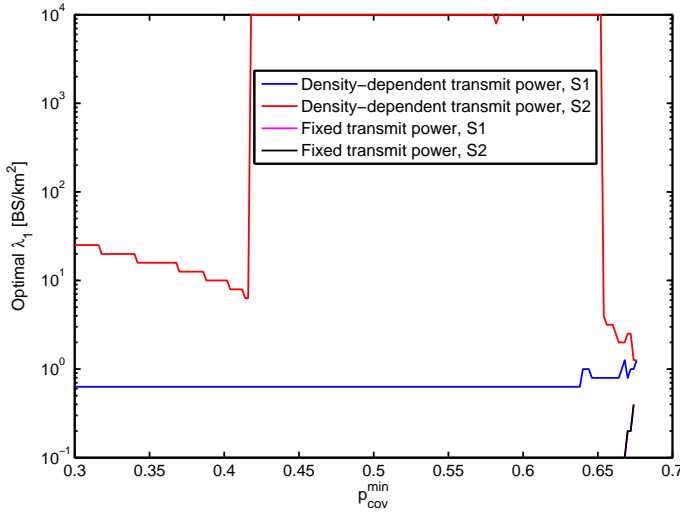


Figure 15. **OP2**: The optimal λ_1 vs. p_{cov}^{\min} in scenarios **S1** and **S2**.

corresponds to a less constraint to the network deployment, as a result choosing proper BS densities becomes much more feasible for mobile operators. The tendency of the red curve, *i.e.*, utilizing a density-dependent transmit power in **S2**, is greatly different from the rest. It is because the corresponding curve of the EE vs. λ_1 and λ_2 as illustrated in Fig. 8 and Fig. 9 is different from that of the rest. It is also noted that the optimal EE is not strictly related to p_{cov}^{\min} , *e.g.*, when $0.43 \leq p_{\text{cov}}^{\min} \leq 0.48$ for the red curve and when $0.30 \leq p_{\text{cov}}^{\min} \leq 0.656$ for the black curve, the optimal EE remains the same. It is because, in these regimes, the optimal λ_1 and λ_2 can guarantee the coverage probability is greater a bit more than the threshold, *i.e.*, p_{cov}^{\min} . To be specific, when we deploy $\lambda_1 = 10^4$ BS/km² and $\lambda_2 = 316.2$ BS/km², the coverage probability is 0.48. And if we set $p_{\text{cov}}^{\min} = 0.43$, the deployment of BSs, *i.e.*, $\lambda_1 = 10^4$ BS/km² and $\lambda_2 = 316.2$ BS/km², can guarantee the minimal coverage probability thus keeps the optimal EE the same. Moreover, when p_{cov}^{\min} is greater than a certain value, *e.g.*, 0.6762 of the red curve, there is no feasible solution to achieve the optimal EE as the QoS of the network, *i.e.*, the coverage probability, can not be guaranteed. The optimal λ_2 is also a decreasing function with respect to p_{cov}^{\min} in Fig. 14. In Fig. 15, when p_{cov}^{\min} is small, the network is not constrained by the coverage performance and deploying more small cell BSs can achieve a better EE. While when p_{cov}^{\min} is larger, mobile operators have to deploy more macrocell BSs to guarantee the network coverage performance, which results in a worse EE. The tendency of the red curve in Fig. 15 is rather different from others. When p_{cov}^{\min} is small, the optimal λ_1 decreases with the increase of p_{cov}^{\min} , then a “flip-flop phenomenon” appears, *i.e.*, the optimal λ_1 jumps to a high value to guarantee the coverage performance and then decreases to a low value to achieve high EE. Besides, comparing Fig. 14 and Fig. 15, it is found that to achieve the optimal EE, an adjustment of λ_1 is needed when p_{cov}^{\min} is small, *i.e.*, $0.30 \leq p_{\text{cov}}^{\min} \leq 0.42$, while λ_2 may keep the same; an adjustment of λ_2 is needed when p_{cov}^{\min} is medium, *i.e.*, $0.42 \leq p_{\text{cov}}^{\min} \leq 0.65$, while λ_1 may keep the same; an adjustment of λ_1 as well as λ_2 is needed when p_{cov}^{\min} is large,

i.e., $p_{\text{cov}}^{\min} \geq 0.65$.

VI. CONCLUSIONS AND FUTURE WORK

In this paper, we investigated network performance of downlink ultra-dense HetNets and study the maximum energy-efficient BS deployment incorporating both NLoS and LoS transmissions. Through analysis, we found that the coverage probability with the MIRP association scheme is better than that with the MARP association scheme and by utilizing a density-dependent transmit power, the coverage probability improves when densities of macrocell BSs and small cell BSs are sparse or medium compared with the HetNets using the fixed transmit power. Moreover, we formulated two optimization problems to achieve the maximum energy-efficient deployment solution with certain minimum service criteria. Simulation results show that there are tradeoffs among the coverage probability, the total power consumption and the EE. In detail, the maximum coverage probability with ideal power consumption is superior to that with practical power consumption when the total power constraint is small and inferior to that with practical power consumption when the total power constraint becomes large. Furthermore, the maximum EE is a decreasing function with respect to the coverage probability constraint. In our future work, networks with idle mode capability and multiple-antennas are also worth further studying.

APPENDIX A: PROOF OF THEOREM 1

The coverage probability in a K -tier HetNet with the MIRP association scheme is defined as follows

$$p_{\text{cov}}^{\text{MIRP}}(\{\lambda_k\}, \{T_k\}) = \Pr \left[\bigcup_{k \in \mathcal{K}, \mathbf{X}_{k,o} \in \Phi_k} \text{SINR}_k(\|\mathbf{X}_{k,o}\|) > T_k \right]. \quad (35)$$

As we consider both NLoS and LoS transmissions, $p_{\text{cov}}^{\text{MIRP}}(\{\lambda_k\}, \{T_k\})$ can be further expressed by

$$\begin{aligned} (35) &= \mathbb{E} \left[\mathbb{I} \left(\bigcup_{k \in \mathcal{K}, \mathbf{X}_{k,o} \in \Phi_k} \text{SINR}_k(\|\mathbf{X}_{k,o}\|) > T_k \right) \right] \\ &= \underbrace{\sum_{k=1}^K \mathbb{E} \left\{ \sum_{\mathbf{X}_{k,o} \in \Phi_k^{\text{NL}}} \left[\mathbb{I}(\text{SINR}_k^{\text{NL}}(\|\mathbf{X}_{k,o}\|) > T_k) \right] \right\}}_I \\ &\quad + \underbrace{\sum_{k=1}^K \mathbb{E} \left\{ \sum_{\mathbf{X}_{k,o} \in \Phi_k^{\text{L}}} \left[\mathbb{I}(\text{SINR}_k^{\text{L}}(\|\mathbf{X}_{k,o}\|) > T_k) \right] \right\}}_{\text{II}}, \quad (36) \end{aligned}$$

where $\mathbb{I}(\cdot)$ is the indicator function, (a) follows from [42, Lemma 1] under the assumption that $T_k \geq 1\forall k$ and the independence between Φ_k^{NL} and Φ_k^{L} , Part I and II in Eq. (36) can be comprehended as the probability that the typical MU is covered by NLoS BSs and LoS BSs, respectively.

Proof: For Part I in Eq. (36), we have

$$\begin{aligned}
 \text{Part I} &\stackrel{(a)}{=} \sum_{k=1}^K \mathbb{E} \left\{ \sum_{\substack{R_{k,o}^{\text{NL}} \in \Phi_k^{\text{NL}} \\ R_{k,o}^{\text{NL}}}} \left[\mathbb{I} \left(\text{SINR}_k^{\text{NL}} \left(\overline{R_{k,o}^{\text{NL}}} \right) > T_k \right) \right] \right\} \\
 &\stackrel{(b)}{=} \sum_{k=1}^K \int_{r=0}^{\infty} \lambda_k^{\text{NL}}(r) \Pr \left[\frac{h_k^{\text{NL}} r^{-\alpha_k^{\text{NL}}}}{\sum_{j=1}^K I_j^{\text{NL}} + \sum_{j=1}^K I_j^{\text{L}} + \eta} > T_k \right] dr \\
 &\stackrel{(c)}{=} \sum_{k=1}^K \int_{r=0}^{\infty} \lambda_k^{\text{NL}}(r) e^{-T_k \eta r^{\alpha_k^{\text{NL}}}} \\
 &\quad \times \prod_{j=1}^K [\mathcal{L}_{I_j^{\text{NL}}}^{\text{MIRP}}(T_k r^{\alpha_k^{\text{NL}}}) \mathcal{L}_{I_j^{\text{L}}}^{\text{MIRP}}(T_k r^{\alpha_k^{\text{NL}}})] dr, \quad (37)
 \end{aligned}$$

where (a) is due to the transformation from Φ_k^{NL} to $\overline{\Phi_k^{\text{NL}}}$, (b) follows from Campbell theorem [20] and variable substitution, i.e., $\overline{R_{k,o}^{\text{NL}}} \rightarrow r$, and $I_j^{\text{NL}} \stackrel{\text{def}}{=} \sum_{i:r_j,i \in \overline{\Phi_j^{\text{NL}}}} h_i^{\text{NL}} r_j^{-\alpha_j^{\text{NL}}}$ and

$I_j^{\text{L}} \stackrel{\text{def}}{=} \sum_{i:r_j,i \in \Phi_j^{\text{L}}} h_i^{\text{L}} r_j^{-\alpha_j^{\text{L}}}$ are the aggregate interference from

NLoS BSs and LoS BSs in the j -th tier, respectively, where $\overline{\Phi_j^{\text{NL}}} = \overline{\Phi_j^{\text{NL}}} \setminus (0, \overline{R_{k,o}^{\text{NL}}}]$, (c) is due to $h_k^{\text{NL}} \sim \exp(1)$, $\mathcal{L}_{I_j^{\text{NL}}}^{\text{MIRP}}(s)$ and $\mathcal{L}_{I_j^{\text{L}}}^{\text{MIRP}}(s)$ denote the Laplace transform of I_j^{NL} and I_j^{L} evaluated at s with the MIRP association scheme, respectively. Using the definition of Laplace transform, we derive $\mathcal{L}_{I_j^{\text{NL}}}^{\text{MIRP}}(s)$ as follows

$$\begin{aligned}
 \mathcal{L}_{I_j^{\text{NL}}}^{\text{MIRP}}(s) &= \mathbb{E}_{I_j^{\text{NL}}} \left[e^{-s I_j^{\text{NL}}} \right] \\
 &\stackrel{(a)}{=} \mathbb{E}_{\overline{\Phi_j^{\text{NL}}}} \left[\prod_{i:r_j,i \in \overline{\Phi_j^{\text{NL}}}} \mathbb{E}_{h_{i,\text{NL}}} \left(e^{-s h_{i,\text{NL}} r_j^{-\alpha_j^{\text{NL}}}} \right) \right] \\
 &\stackrel{(b)}{=} \exp \left[\int_{y=0}^{\infty} \left(\frac{1}{1 + s y^{-\alpha_j^{\text{NL}}}} - 1 \right) \lambda_j^{\text{NL}}(y) dy \right] \\
 &= \exp \left[-s^{1/\alpha_j^{\text{NL}}} \int_{y=0}^{\infty} \frac{\lambda_j^{\text{NL}}(y s^{1/\alpha_j^{\text{NL}}})}{1 + y^{\alpha_j^{\text{NL}}}} dy \right], \quad (38)
 \end{aligned}$$

where (a) follows from the independence between the fading random variables (RVs), i.e., h_j^{NL} , (b) follows from probability generating functional (PGFL) of PPP [20].

Similarly, $\mathcal{L}_{I_j^{\text{L}}}^{\text{MIRP}}(s)$ is obtained as follows

$$\mathcal{L}_{I_j^{\text{L}}}^{\text{MIRP}}(s) = \exp \left[-s^{1/\alpha_j^{\text{L}}} \int_{y=0}^{\infty} \frac{\lambda_j^{\text{L}}(y s^{1/\alpha_j^{\text{L}}})}{1 + y^{\alpha_j^{\text{L}}}} dy \right], \quad (39)$$

Using a similar approach compared with Part I, Part II can also be easily obtained as follows

$$\begin{aligned}
 \text{Part II} &= \sum_{k=1}^K \int_{t=0}^{\infty} \lambda_k^{\text{L}}(r) e^{-T_k \eta r^{\alpha_k^{\text{L}}}} \\
 &\quad \times \prod_{j=1}^K [\mathcal{L}_{I_j^{\text{NL}}}^{\text{MIRP}}(T_k r^{\alpha_k^{\text{L}}}) \mathcal{L}_{I_j^{\text{L}}}^{\text{MIRP}}(T_k r^{\alpha_k^{\text{L}}})] dr, \quad (40)
 \end{aligned}$$

where $\mathcal{L}_{I_j^{\text{NL}}}^{\text{MIRP}}(s)$ and $\mathcal{L}_{I_j^{\text{L}}}^{\text{MIRP}}(s)$ are defined in Eq. (38) and Eq. (39), respectively. Then, the proof is completed. ■

APPENDIX B: PROOF OF THEOREM 2

Using the law of total probability, we can calculate coverage probability $p_{\text{cov}}^{\text{MARP}}(\{\lambda_k\}, \{T_k\})$ as

$$\begin{aligned}
 p_{\text{cov}}^{\text{MARP}}(\{\lambda_k\}, \{T_k\}) &= \sum_{k=1}^K p_k^{\text{NL}}(\{\lambda_k\}, \{T_k\}) \\
 &\quad + \sum_{k=1}^K p_k^{\text{L}}(\{\lambda_k\}, \{T_k\}), \quad (41)
 \end{aligned}$$

where the first part and the second part on the right side of the equation denote the conditional coverage probability that the typical MU is in the coverage of NLoS BSs and LoS BSs, respectively, by observing that the two events are disjoint. Given that the typical MU is served by an NLoS BS and an the maximum average received power is denote by $\mathcal{P}_k^{\text{NL}}$, i.e., $\mathcal{P}_k^{\text{NL}} = \max(P_{k,i}^{\text{NL}})$. Then

$$\begin{aligned}
 &p_k^{\text{NL}}(\{\lambda_k^{\text{NL}}\}, \{T_k\}) \\
 &= \Pr \left[(\text{SINR}_k^{\text{NL}} > T_k) \cap \left(\bigcap_{j \in \mathcal{K}} \{\mathcal{P}_k^{\text{NL}} > \mathcal{P}_j^{\text{L}}\}, \right. \right. \\
 &\quad \left. \bigcap_{j \in \mathcal{K} \setminus k} \{\mathcal{P}_k^{\text{NL}} > \mathcal{P}_j^{\text{NL}}\} \right) \cap \mathcal{Y}_k^{\text{NL}} \Big] \\
 &= \mathbb{E}_{\mathcal{Y}_k^{\text{NL}}} \left\{ \Pr \left[\text{SINR}_k^{\text{NL}} > T_k \mid \left(\bigcap_{j \in \mathcal{K}} \{\mathcal{P}_k^{\text{NL}} > \mathcal{P}_j^{\text{L}}\}, \right. \right. \right. \\
 &\quad \left. \bigcap_{j \in \mathcal{K} \setminus k} \{\mathcal{P}_k^{\text{NL}} > \mathcal{P}_j^{\text{NL}}\} \right) \cap \mathcal{Y}_k^{\text{NL}} \Big] \right. \\
 &\quad \left. \times \underbrace{\Pr \left[\bigcap_{j \in \mathcal{K}} \{\mathcal{P}_k^{\text{NL}} > \mathcal{P}_j^{\text{L}}\}, \bigcap_{j \in \mathcal{K} \setminus k} \{\mathcal{P}_k^{\text{NL}} > \mathcal{P}_j^{\text{NL}}\} \mid \mathcal{Y}_k^{\text{NL}} \right]}_1 \right\}, \quad (42)
 \end{aligned}$$

where $\mathcal{Y}_k^{\text{NL}}$ is the equivalent distance between the typical MU and the BS providing the maximum average received power to the typical MU in Φ_k^{NL} , i.e., $\mathcal{Y}_k^{\text{NL}} = \arg \max_{R_{k,i}^{\text{NL}} \in \overline{\Phi_k^{\text{NL}}}} (R_{k,i}^{\text{NL}})^{-\alpha_k^{\text{NL}}}$,

and also note that $\mathcal{P}_k^{\text{NL}} = (\mathcal{Y}_k^{\text{NL}})^{-\alpha_k^{\text{NL}}}$. We label the formulas before and after the product sign “ \times ” as Part II and Part I, respectively. For Part I,

$$\begin{aligned}
 &\Pr \left[\bigcap_{j \in \mathcal{K}} \{\mathcal{P}_k^{\text{NL}} > \mathcal{P}_j^{\text{L}}\}, \bigcap_{j \in \mathcal{K} \setminus k} \{\mathcal{P}_k^{\text{NL}} > \mathcal{P}_j^{\text{NL}}\} \mid \mathcal{Y}_k^{\text{NL}} \right] \\
 &= \prod_{j \in \mathcal{K}} \Pr \left[\mathcal{P}_k^{\text{NL}} > \mathcal{P}_j^{\text{L}} \mid \mathcal{Y}_k^{\text{NL}} \right] \prod_{j \in \mathcal{K} \setminus k} \Pr \left[\mathcal{P}_k^{\text{NL}} > \mathcal{P}_j^{\text{NL}} \mid \mathcal{Y}_k^{\text{NL}} \right] \\
 &= \prod_{j \in \mathcal{K}} \Pr \left[(\mathcal{Y}_k^{\text{NL}})^{-\alpha_k^{\text{NL}}} > (\mathcal{Y}_j^{\text{L}})^{-\alpha_j^{\text{L}}} \mid \mathcal{Y}_k^{\text{NL}} \right] \\
 &\quad \times \prod_{j \in \mathcal{K} \setminus k} \Pr \left[(\mathcal{Y}_k^{\text{NL}})^{-\alpha_k^{\text{NL}}} > (\mathcal{Y}_j^{\text{NL}})^{-\alpha_j^{\text{NL}}} \mid \mathcal{Y}_k^{\text{NL}} \right] \\
 &\stackrel{(a)}{=} \prod_{j \in \mathcal{K}} \exp \left[-\Lambda_j^{\text{L}} \left([0, (\mathcal{Y}_k^{\text{NL}})^{\alpha_k^{\text{NL}}/\alpha_j^{\text{L}}}] \right) \right] \\
 &\quad \times \prod_{j \in \mathcal{K} \setminus k} \exp \left[-\Lambda_j^{\text{NL}} \left([0, (\mathcal{Y}_k^{\text{NL}})^{\alpha_k^{\text{NL}}/\alpha_j^{\text{NL}}}] \right) \right] \\
 &= \exp \left[-\sum_{j \in \mathcal{K}} \Lambda_j^{\text{L}} \left([0, (\mathcal{Y}_k^{\text{NL}})^{\alpha_k^{\text{NL}}/\alpha_j^{\text{L}}}] \right) \right. \\
 &\quad \left. - \sum_{j \in \mathcal{K} \setminus k} \Lambda_j^{\text{NL}} \left([0, (\mathcal{Y}_k^{\text{NL}})^{\alpha_k^{\text{NL}}/\alpha_j^{\text{NL}}}] \right) \right], \quad (43)
 \end{aligned}$$

where \mathcal{Y}_k^L , similar to the definition of \mathcal{Y}_k^{NL} , is the equivalent distance between the typical MU and the BS providing the maximum average received power to the typical MU in Φ_k^L , i.e., $\mathcal{Y}_k^L = \arg \max_{R_{k,i}^L \in \Phi_k^L} (\overline{R_{k,i}^L})^{-\alpha_k^L}$, and also note that $\mathcal{P}_k^L = (\mathcal{Y}_k^L)^{-\alpha_k^L}$, and (a) follows from the void probability of a PPP.

For Part II, we know that $\text{SINR}_k^{NL} = \frac{h_k^{NL} \mathcal{P}_k^{NL}}{\sum_{j=1}^K I_j^{NL} + \sum_{j=1}^K I_j^L + \eta}$. The conditional coverage probability can be derived as follows

$$\begin{aligned} \text{Part II} &\stackrel{(a)}{=} \Pr \left[\frac{h_k^{NL} (\mathcal{Y}_k^{NL})^{-\alpha_k^{NL}}}{\sum_{j=1}^K I_j^{NL} + \sum_{j=1}^K I_j^L + \eta} > T_k \mid \mathbf{E} \right] \\ &= \Pr [h_k^{NL} > T_k (\mathcal{Y}_k^{NL})^{\alpha_k^{NL}} \left(\sum_{j=1}^K I_j^{NL} + \sum_{j=1}^K I_j^L + \eta \right) \mid \mathbf{E}] \\ &\stackrel{(b)}{=} e^{-T_k \eta r^{\alpha_k^{NL}}} \prod_{j=1}^K [\mathcal{L}_{I_j^{NL}}^{\text{MARPI}}(T_k r^{\alpha_k^{NL}}) \mathcal{L}_{I_j^L}^{\text{MARPI}}(T_k r^{\alpha_k^{NL}})], \quad (44) \end{aligned}$$

where in (a) event $\mathbf{E} \stackrel{\text{def}}{=} \left(\bigcap_{j \in \mathcal{K}} \{ \mathcal{P}_k^{NL} > \mathcal{P}_j^L \}, \bigcap_{j \in \mathcal{K} \setminus k} \{ \mathcal{P}_k^{NL} > \mathcal{P}_j^{NL} \} \right) \cap \mathcal{Y}_k^{NL}$, (b) follows from $h_k^{NL} \sim \exp(1)$ and variable substitution, i.e., $\mathcal{Y}_k^{NL} \rightarrow r$, $\mathcal{L}_{I_j^{NL}}^{\text{ave}}(s)$ and $\mathcal{L}_{I_j^L}^{\text{ave}}(s)$ denote the Laplace transform of I_j^{NL} and I_j^L evaluated at s with the MARP association scheme, respectively. Like Appendix A, we derive $\mathcal{L}_{I_j^{NL}}^{\text{MARPI}}(s)$ as follows

$$\begin{aligned} \mathcal{L}_{I_j^{NL}}^{\text{MARPI}}(s) &= \mathbb{E}_{I_j^{NL}} [e^{-s I_j^{NL}}] \\ &= \mathbb{E}_{\Phi_j^{NL}} \left[\prod_{i: r_{j,i} \in \widehat{\Phi}_j^{NL}} \frac{1}{1 + s r_{j,i}^{-\alpha_j^{NL}}} \right] \\ &\stackrel{(a)}{=} \exp \left[- \int_{y=(\mathcal{Y}_k^{NL})^{\alpha_k^{NL}/\alpha_j^{NL}}}^{\infty} \frac{\lambda_j^{NL}(y)}{1 + y^{\alpha_j^{NL}}/s} dy \right], \quad (45) \end{aligned}$$

where $\widehat{\Phi}_j^{NL} = \overline{\Phi}_j^{NL} \setminus (0, \mathcal{Y}_k^{NL}]$ and in (a) the lower limit of integral is $(\mathcal{Y}_k^{NL})^{\alpha_k^{NL}/\alpha_j^{NL}}$ which guarantees that $\mathcal{P}_k^{NL} > \mathcal{P}_j^{NL}, \forall j \in \mathcal{K} \setminus k$ in event \mathbf{E} is true. Similarly, $\mathcal{L}_{I_j^L}^{\text{MARPI}}(s)$ is calculated by

$$\begin{aligned} \mathcal{L}_{I_j^L}^{\text{MARPI}}(s) &= \mathbb{E}_{I_j^L} [e^{-s I_j^L}] \\ &\stackrel{(a)}{=} \exp \left[- \int_{y=(\mathcal{Y}_k^L)^{\alpha_k^L/\alpha_j^L}}^{\infty} \frac{\lambda_j^L(y)}{1 + y^{\alpha_j^L}/s} dy \right], \quad (46) \end{aligned}$$

where in (a) the lower limit of integral is $(\mathcal{Y}_k^L)^{\alpha_k^L/\alpha_j^L}$ which guarantees that $\{ \mathcal{P}_k^L > \mathcal{P}_j^L \}, \forall j \in \mathcal{K}$ in event \mathbf{E} is true.

Finally, note that the value of $p_k^{NL}(\{\lambda_k\}, \{T_k\})$ in Eq. (42) should be calculated by taking the expectation with respect to \mathcal{Y}_k^{NL} in terms of its PDF, which is given by

$$f_{\mathcal{Y}_k^{NL}}(\varepsilon) = \lambda_k^{NL}(\varepsilon) \exp[-\Lambda_k^{NL}([0, \varepsilon])] \quad (47)$$

as in [31]. By substituting Eq. (43), (44), (45), (46), and (47) into Eq. (42), we can derive the conditional probability $p_k^{NL}(\{\lambda_k\}, \{T_k\})$. Given that the typical MU is connected to a LoS BS, the conditional coverage probability $p_k^L(\{\lambda_k\}, \{T_k\})$ can be derived using the similar way as the above. Thus the proof is completed.

APPENDIX C: PROOF OF COROLLARY 5

By comparing $p_{\text{cov}}^{\text{MIRP}}(\{\lambda_k\}, \{T_k\})$ and $p_{\text{cov}}^{\text{MARP}}(\{\lambda_k\}, \{T_k\})$ in Theorem 1 and 2, it is noticed that the difference between them lies in the Laplace transform $e^{-\sum_{j=1}^K [\Lambda_j^L([0, r^{\alpha_k^L/\alpha_j^L}]) + \Lambda_j^{NL}([0, r^{\alpha_k^L/\alpha_j^{NL}}])]}$ and the term $e^{-\sum_{j=1}^K [\Lambda_j^L([0, r^{\alpha_k^L/\alpha_j^L}]) + \Lambda_j^{NL}([0, r^{\alpha_k^L/\alpha_j^{NL}}])]}$. Thus, we prove this corollary by taking the coverage probability for a typical MU which is served LoS BSs for an example.

$$\begin{aligned} p_{\text{cov}}^{\text{MIRP}}(\{\lambda_k\}, \{T_k\}) &> p_{\text{cov}}^{\text{MARP}}(\{\lambda_k\}, \{T_k\}) \\ \iff e^{-\sum_{j=1}^K [\Lambda_j^L([0, r^{\alpha_k^L/\alpha_j^L}]) + \Lambda_j^{NL}([0, r^{\alpha_k^L/\alpha_j^{NL}}])]} & \\ \times \prod_{j=1}^K [\mathcal{L}_{I_j^{NL}}^{\text{MARP2}}(T_k r^{\alpha_k^L}) \mathcal{L}_{I_j^L}^{\text{MARP2}}(T_k r^{\alpha_k^L})] / & \\ \prod_{j=1}^K [\mathcal{L}_{I_j^{NL}}^{\text{MIRP}}(T_k r^{\alpha_k^L}) \mathcal{L}_{I_j^L}^{\text{MIRP}}(T_k r^{\alpha_k^L})] &< 1 \\ \iff \exp \left[- \sum_{j=1}^K [\Lambda_j^L([0, r^{\alpha_k^L/\alpha_j^L}]) + \Lambda_j^{NL}([0, r^{\alpha_k^L/\alpha_j^{NL}}])] \right. & \\ \left. - \int_0^{r^{\alpha_k^L/\alpha_j^L}} \frac{\lambda_j^L(y)}{1 + y^{\alpha_j^L}/T_k r^{\alpha_k^L}} dy \right. & \\ \left. - \int_0^{r^{\alpha_k^L/\alpha_j^{NL}}} \frac{\lambda_j^{NL}(y)}{1 + y^{\alpha_j^{NL}}/T_k r^{\alpha_k^L}} dy \right] &< 1 \\ \iff \Lambda_j^L([0, r^{\alpha_k^L/\alpha_j^L}]) > \int_0^{r^{\alpha_k^L/\alpha_j^L}} \frac{\lambda_j^L(y)}{1 + y^{\alpha_j^L}/T_k r^{\alpha_k^L}} dy, & \\ \text{and } \Lambda_j^{NL}([0, r^{\alpha_k^L/\alpha_j^{NL}}]) > \int_0^{r^{\alpha_k^L/\alpha_j^{NL}}} \frac{\lambda_j^{NL}(y)}{1 + y^{\alpha_j^{NL}}/T_k r^{\alpha_k^L}} dy & \\ \iff \lambda_j^L(y) > \frac{\lambda_j^L(y)}{1 + y^{\alpha_j^L}/T_k r^{\alpha_k^L}}, & \\ \text{and } \lambda_j^{NL}(y) > \frac{\lambda_j^{NL}(y)}{1 + y^{\alpha_j^{NL}}/T_k r^{\alpha_k^L}}. & \quad (48) \end{aligned}$$

The proof is completed.

REFERENCES

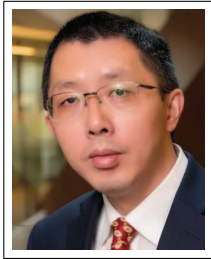
- [1] X. Ge, S. Tu, G. Mao, C. X. Wang, and T. Han, "5g ultra-dense cellular networks," *IEEE Wireless Commun.*, vol. 23, no. 1, pp. 72–79, Feb. 2016.
- [2] D. Lopez-Perez, M. Ding, H. Claussen, and A. H. Jafari, "Towards 1 gbps/ue in cellular systems: Understanding ultra-dense small cell deployments," *IEEE Commun. Surv. Tut.*, vol. 17, no. 4, pp. 2078–2101, Nov. 2015.
- [3] J. G. Andrews, F. Baccelli, and R. K. Ganti, "A tractable approach to coverage and rate in cellular networks," *IEEE Trans. Commun.*, vol. 59, no. 11, pp. 3122–3134, Nov. 2011.
- [4] D. Liu, L. Wang, Y. Chen, M. El-kashlan, K. K. Wong, R. Schober, and L. Hanzo, "User association in 5g networks: A survey and an outlook," *IEEE Commun. Surveys Tuts.*, vol. 18, no. 2, pp. 1018–1044, Secondquarter 2016.
- [5] D. Bethanabhotla, O. Y. Bursalioğlu, H. C. Papadopoulos, and G. Caire, "Optimal user-cell association for massive mimo wireless networks," *IEEE Trans. Wireless Commun.*, vol. 15, no. 3, pp. 1835–1850, Mar. 2016.

- [6] N. Wang, E. Hossain, and V. K. Bhargava, "Joint downlink cell association and bandwidth allocation for wireless backhauling in two-tier hetnets with large-scale antenna arrays," *IEEE Trans. Wireless Commun.*, vol. 15, no. 5, pp. 3251–3268, Jan. 2016.
- [7] C. Yang, Y. Yao, Z. Chen, and B. Xia, "Analysis on cache-enabled wireless heterogeneous networks," *IEEE Trans. Wireless Commun.*, vol. 15, no. 1, pp. 131–145, Aug. 2016.
- [8] H. M. Wang, T. X. Zheng, J. Yuan, D. Towsley, and M. H. Lee, "Physical layer security in heterogeneous cellular networks," *IEEE Trans. Commun.*, vol. 64, no. 3, pp. 1204–1219, Jan. 2016.
- [9] I. Humar, X. Ge, L. Xiang, M. Jo, M. Chen, and J. Zhang, "Rethinking energy efficiency models of cellular networks with embodied energy," *IEEE Network*, vol. 25, no. 2, pp. 40–49, Mar. 2011.
- [10] A. Shojaefard, K. K. Wong, K. Hamdi, E. Alsusa, D. K. C. So, and J. Tang, "Stochastic geometric analysis of energy-efficient dense cellular networks," *IEEE Access*, vol. PP, no. 99, pp. 1–1, Dec. 2016.
- [11] Y. Niu, C. Gao, Y. Li, L. Su, D. Jin, Y. Zhu, and D. O. Wu, "Energy-efficient scheduling for mmwave backhauling of small cells in heterogeneous cellular networks," *IEEE Trans. Veh. Technol.*, vol. 66, no. 3, pp. 2674–2687, Mar. 2017.
- [12] A. Shahid, K. S. Kim, E. D. Poorter, and I. Moerman, "Self-organized energy-efficient cross-layer optimization for device to device communication in heterogeneous cellular networks," *IEEE Access*, vol. 5, pp. 1117–1128, Mar. 2017.
- [13] J. Wu, B. Cheng, M. Wang, and J. Chen, "Energy-efficient bandwidth aggregation for delay-constrained video over heterogeneous wireless networks," *IEEE J. Sel. Areas Commun.*, vol. 35, no. 1, pp. 30–49, Jan. 2017.
- [14] K. Yang, S. Martin, D. Quadri, J. Wu, and G. Feng, "Energy-efficient downlink resource allocation in heterogeneous ofdma networks," *IEEE Trans. Veh. Technol.*, vol. 66, no. 6, pp. 5086–5098, Jun. 2017.
- [15] K. Zhang, Y. Mao, S. Leng, Q. Zhao, L. Li, X. Peng, L. Pan, S. Maharjan, and Y. Zhang, "Energy-efficient offloading for mobile edge computing in 5g heterogeneous networks," *IEEE Access*, vol. 4, pp. 5896–5907, Aug. 2016.
- [16] M. Ding, P. Wang, D. Lopez-Perez, G. Mao, and Z. Lin, "Performance impact of los and nlos transmissions in dense cellular networks," *IEEE Trans. Wireless Commun.*, vol. 15, no. 3, pp. 2365–2380, Mar. 2016.
- [17] M. D. Renzo, "Stochastic geometry modeling and analysis of multi-tier millimeter wave cellular networks," *IEEE Trans. Wireless Commun.*, vol. 14, no. 9, pp. 5038–5057, Sep. 2015.
- [18] S. Singh, M. N. Kulkarni, A. Ghosh, and J. G. Andrews, "Tractable model for rate in self-backhauled millimeter wave cellular networks," *IEEE J. Sel. Areas Commun.*, vol. 33, no. 10, pp. 2196–2211, Oct. 2015.
- [19] T. Bai and R. W. Heath, "Coverage and rate analysis for millimeter-wave cellular networks," *IEEE Trans. Wireless Commun.*, vol. 14, no. 2, pp. 1100–1114, Feb. 2015.
- [20] M. Haenggi, *Stochastic Geometry for Wireless Networks*. Cambridge University Press, 2012.
- [21] N. Blaunstein and M. Levin, "Parametric model of uhf/l-wave propagation in city with randomly distributed buildings," in *Proc. IEEE Antennas and Propagation Society International Symposium*, vol. 3, Jun. 1998, pp. 1684–1687.
- [22] T. Bai, R. Vaze, and R. W. Heath, "Analysis of blockage effects on urban cellular networks," *IEEE Trans. Wireless Commun.*, vol. 13, no. 9, pp. 5070–5083, Sep. 2014.
- [23] J. Liu, M. Sheng, L. Liu, and J. Li, "Effect of densification on cellular network performance with bounded pathloss model," *IEEE Commun. Lett.*, vol. 21, no. 2, pp. 346–349, Feb. 2017.
- [24] A. AlAmmouri, J. G. Andrews, and F. Baccelli, "Sinr and throughput of dense cellular networks with stretched exponential path loss," Mar. 2017. Available at: <https://arxiv.org/abs/1703.08246>.
- [25] M. Ding, D. Lopez-Perez, G. Mao, and Z. Lin, "Performance impact of idle mode capability on dense small cell networks," Mar. 2017. Available at: <https://arxiv.org/abs/1609.07710v4>.
- [26] B. Yang, G. Mao, X. Ge, and T. Han, "A new cell association scheme in heterogeneous networks," in *Proc. IEEE ICC 2015*, June 2015, pp. 5627–5632.
- [27] S. N. Chiu, D. Stoyan, W. S. Kendall, and J. Mecke, *Stochastic geometry and its applications*. John Wiley & Sons, 2013.
- [28] B. Wei and L. Ben, "Structured spectrum allocation and user association in heterogeneous cellular networks," in *Proc. IEEE INFOCOM 2014*, pp. 1069–1077.
- [29] J. Peng, P. Hong, and K. Xue, "Energy-aware cellular deployment strategy under coverage performance constraints," *IEEE Trans. Wireless Commun.*, vol. 14, no. 1, pp. 69–80, Jan. 2015.
- [30] H. ElSawy, A. Sultan-Salem, M. S. Alouini, and M. Z. Win, "Modeling and analysis of cellular networks using stochastic geometry: A tutorial," *IEEE Commun. Surveys Tuts.*, vol. 19, no. 1, pp. 167–203, Firstquarter 2017.
- [31] B. Yang, G. Mao, M. Ding, X. Ge, and X. Tao, "Dense small cell networks: From noise-limited to dense interference-limited," *IEEE Trans. Veh. Technol.*, vol. PP, no. 99, pp. 1–1, Jan. 2018.
- [32] X. Ge, B. Yang, J. Ye, G. Mao, C. X. Wang, and T. Han, "Spatial spectrum and energy efficiency of random cellular networks," *IEEE Trans. Commun.*, vol. 63, no. 3, pp. 1019–1030, Mar. 2015.
- [33] D. Cao, S. Zhou, and Z. Niu, "Optimal combination of base station densities for energy-efficient two-tier heterogeneous cellular networks," *IEEE Trans. Wireless Commun.*, vol. 12, no. 9, pp. 4350–4362, Sep. 2013.
- [34] X. Ge, B. Yang, J. Ye, G. Mao, and Q. Li, "Performance analysis of poisson-voronoi tessellated random cellular networks using markov chains," in *Proc. IEEE Globecom 2014*, Dec. 2014, pp. 4635–4640.
- [35] R. P. Brent, *Algorithms for Minimization Without Derivatives*. Englewood Cliffs, NJ, USA: Prentice-Hall, 1973.
- [36] W. H. Press, S. A. Teukolsky, W. T. Vetterling, and B. P. Flannery, *Numerical Recipes: The Art of Scientific Computing*. 3rd ed. Cambridge, U.K.: Cambridge Univ. Press, 2007.
- [37] 3GPP, "Tr 36.828 (v11.0.0): Further enhancements to lte time division duplex (tdd) for downlink-uplink (dl-ul) interference management and traffic adaptation," Jun. 2012.
- [38] B. Yang, G. Mao, X. Ge, H. H. Chen, T. Han, and X. Zhang, "Coverage analysis of heterogeneous cellular networks in urban areas," in *Proc. IEEE ICC*, May 2016, pp. 1–6.
- [39] X. Ge, L. Pan, Q. Li, G. Mao, and S. Tu, "Multipath cooperative communications networks for augmented and virtual reality transmission," *IEEE Trans. Multimedia*, vol. 19, no. 10, pp. 2345–2358, Oct. 2017.
- [40] X. Ge, J. Ye, Y. Yang, and Q. Li, "User mobility evaluation for 5g small cell networks based on individual mobility model," *IEEE J. Sel. Areas Commun.*, vol. 34, no. 3, pp. 528–541, Mar. 2016.
- [41] X. Ge, J. Martínez-Bauset, V. Casares-Giner, B. Yang, J. Ye, and M. Chen, "Modelling and performance analysis of different access schemes in two-tier wireless networks," in *Proc. IEEE Globecom 2013*, Dec. 2013, pp. 4402–4407.
- [42] H. S. Dhillon, R. K. Ganti, F. Baccelli, and J. G. Andrews, "Modeling and analysis of k-tier downlink heterogeneous cellular networks," *IEEE J. Sel. Areas Commun.*, vol. 30, no. 3, pp. 550–560, Apr. 2012.



Bin Yang (S'13) is currently pursuing the Ph.D. degree at School of Electronic Information and Communications, Huazhong University of Science and Technology, Wuhan, China. His research interests include queuing theory, stochastic geometry, ultra-dense networks, green communications and network optimization.

He was a visiting student at University of Technology, Sydney from January 2015 to June 2015 and January 2016 to January 2017. He has received the Best Paper Award from European Wireless 2016 and Best 50 Papers from IEEE Globecom 2014. He has also received the student travel grant from IEEE ICC 2017.



Guoqiang Mao (S'98-M'02-SM'08-F'18) joined the University of Technology Sydney in February 2014 as Professor of Wireless Networking and Director of Center for Real-time Information Networks. Before that, he was with the School of Electrical and Information Engineering, the University of Sydney. He has published about 200 papers in international conferences and journals, which have been cited more than 5000 times. He is an editor of the IEEE Transactions on Wireless Communications (since 2014), IEEE Transactions on Vehicular Technology (since 2010) and received "Top Editor" award for outstanding contributions to the IEEE Transactions on Vehicular Technology in 2011, 2014 and 2015. He is a co-chair of IEEE Intelligent Transport Systems Society Technical Committee on Communication Networks. He has served as a chair, co-chair and TPC member in a large number of international conferences. He is a Fellow of IEEE and IET. His research interest includes intelligent transport systems, applied graph theory and its applications in telecommunications, Internet of Things, wireless sensor networks, wireless localization techniques and network performance analysis.



Ming Ding (M'12-SM'17) received the B.S. and M.S. degrees (with first class Hons.) in electronics engineering from Shanghai Jiao Tong University (SJTU), Shanghai, China, and the Doctor of Philosophy (Ph.D.) degree in signal and information processing from SJTU, in 2004, 2007, and 2011, respectively. From April 2007 to September 2014, he worked at Sharp Laboratories of China in Shanghai, China as a Researcher/Senior Researcher/Principal Researcher. He also served as the Algorithm Design Director and Programming Director for a system-level simulator of future telecommunication networks in Sharp Laboratories of China for more than 7 years. Currently, he is a senior research scientist at Data61, CSIRO, in Sydney, NSW, Australia. He has authored more than 60 papers in IEEE journals and conferences, all in recognized venues, and about 20 3GPP standardization contributions, as well as a Springer book "Multi-point Cooperative Communication Systems: Theory and Applications". Also, as the first inventor, he holds 15 CN, 7 JP, 3 US, 2 KR patents and co-authored another 100+ patent applications on 4G/5G technologies. He is or has been Guest Editor/Co-Chair/Co-Tutor/TPC member of several IEEE top-tier journals/conferences, e.g., the IEEE Journal on Selected Areas in Communications, the IEEE Communications Magazine, and the IEEE Globecom Workshops, etc. For his inventions and publications, he was the recipient of the President's Award of Sharp Laboratories of China in 2012, and served as one of the key members in the 4G/5G standardization team when it was awarded in 2014 as Sharp Company Best Team: LTE 2014 Standardization Patent Portfolio.



Xiaohu Ge (M'09-SM'11) received the Ph.D. degree in communication and information engineering from the Huazhong University of Science and Technology (HUST), Wuhan, China, in 2003. Since 2005, he has been with HUST, where he is currently a Full Professor with the School of Electronic Information and Communications. He is an Adjunct Professor with Faculty of Engineering and Information Technology, University of Technology Sydney, Ultimo, NSW, Australia. He is the Director of the China International Joint Research Center of

Green Communications and Networking. Before joining the HUST in 2005, he was as a Researcher with Ajou University, Suwon, South Korea and the Politecnico Di Torino, Torino, Italy, from January 2004 to October 2005. His research interests include the area of mobile communications, traffic modeling in wireless networks, green communications, and interference modeling in wireless communications. He has authored or coauthored about 200 papers in refereed journals and conference proceedings and has been granted about 15 patents in China. He has been actively involved in organizing more than ten international conferences since 2005. He was the General Chair for the 2015 IEEE International Conference on Green Computing and Communications. He is an Editor for the IEEE Wireless Communications, IEEE Transactions on Vehicular Technology, IEEE Transactions on Green Communications and Networking, etc.



Xuan Yang received his Bachelor's degree in communication and information systems from Hunan University in 2017. He is currently working toward his Master's degree in Huazhong University of Science and Technology. His research interests include wireless communication networks and 5G mobile communication systems.